Supporting Information

Effective N-methylation of nitroarenes with methanol catalyzed by a functionalized NHC-based iridium catalyst: a green approach to N-methyl amines

Miguel González-Lainez,[†] M. Victoria Jiménez,[*,†] Vincenzo Passarelli[†,‡] and Jesús J. Pérez-Torrente[*,†]

[†] *Departamento de Química Inorgánica – Instituto de Síntesis Química y Catálisis Homogénea-ISQCH, Universidad de Zaragoza – CSIC, C/ Pedro Cerbuna 12, 50009 Zaragoza, Spain*

[‡] *Centro Universitario de la Defensa, Ctra Huesca S/N 50090 Zaragoza, Spain*

Contents

1.- ^{1}H and $^{13}C\{^{1}H\}$ NMR spectra of compounds 1-4.

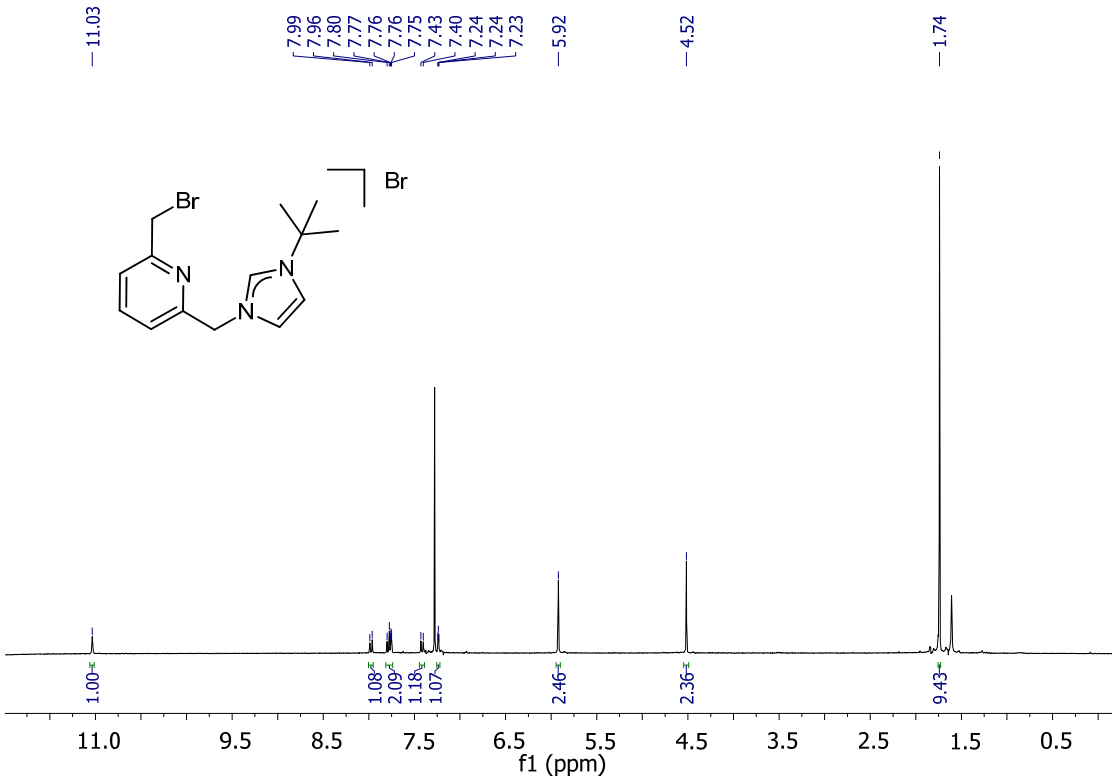

Figure S1. ^{1}H NMR spectrum of [^{t}BuHImCH$_2$PyCH$_2$Br]Br (**1**) registered in CDCl$_3$.

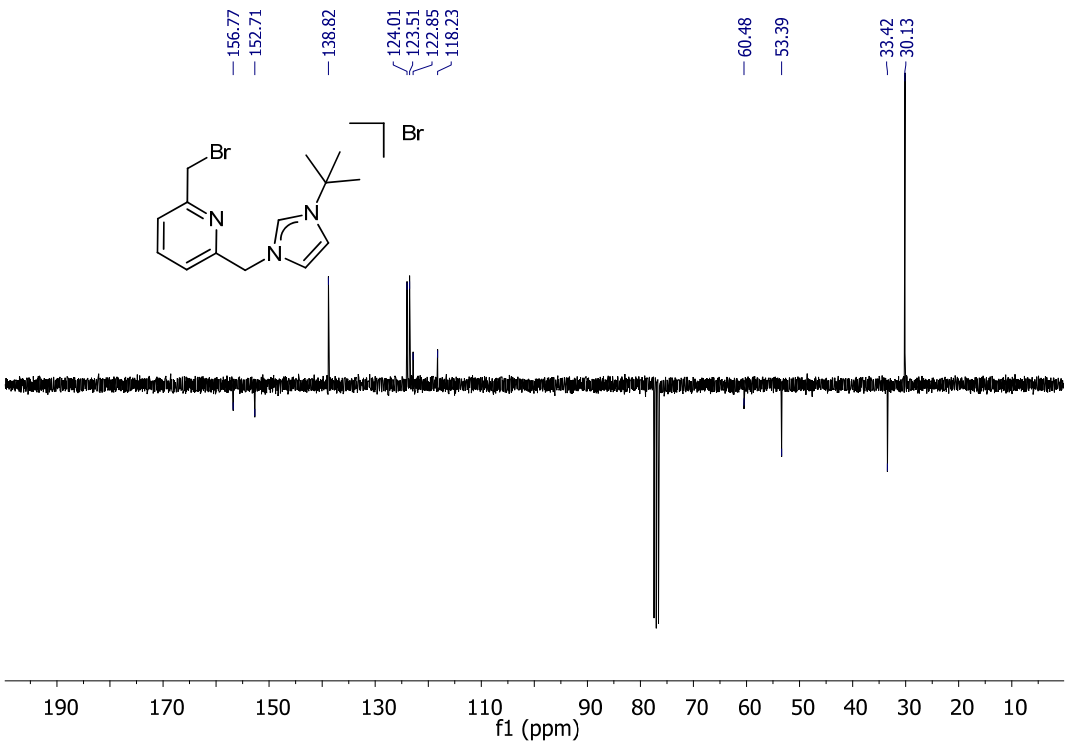

Figure S2. ^{13}C NMR APT of [^{t}BuHImCH$_2$PyCH$_2$Br]Br (**1**) registered in CDCl$_3$.

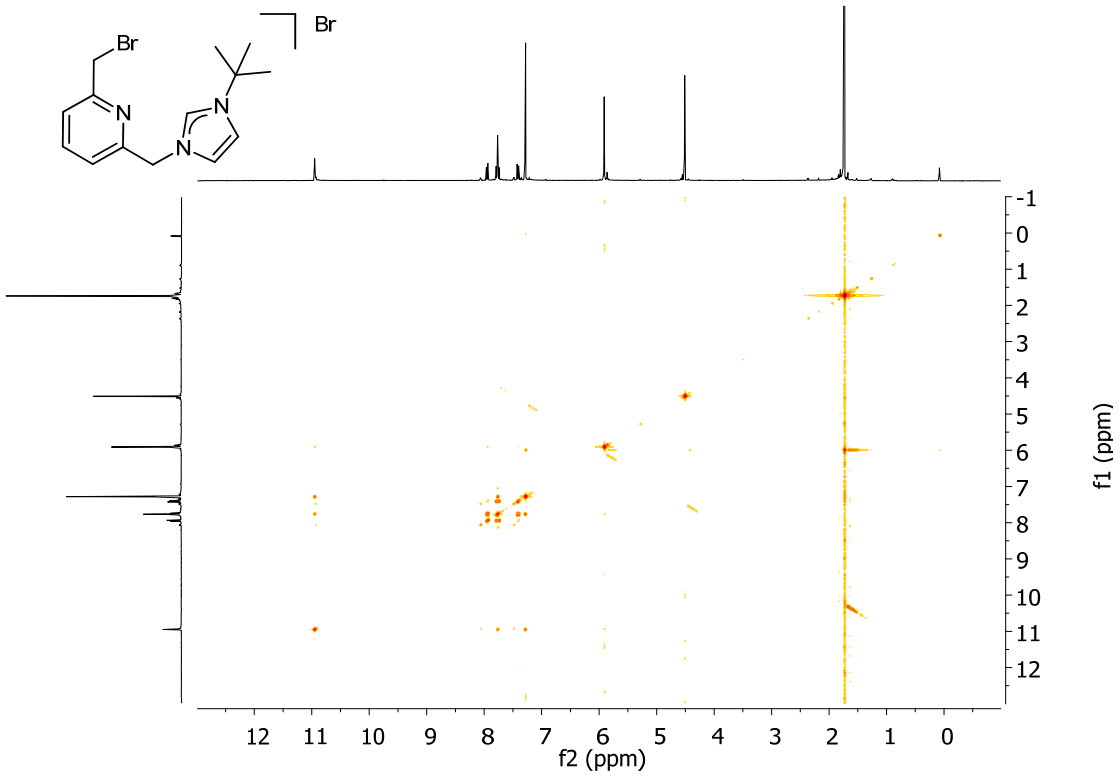

Figure S3. ^{1}H-^{1}H COSY of [^{t}BuHImCH$_2$PyCH$_2$Br]Br (**1**) registered in CDCl$_3$.

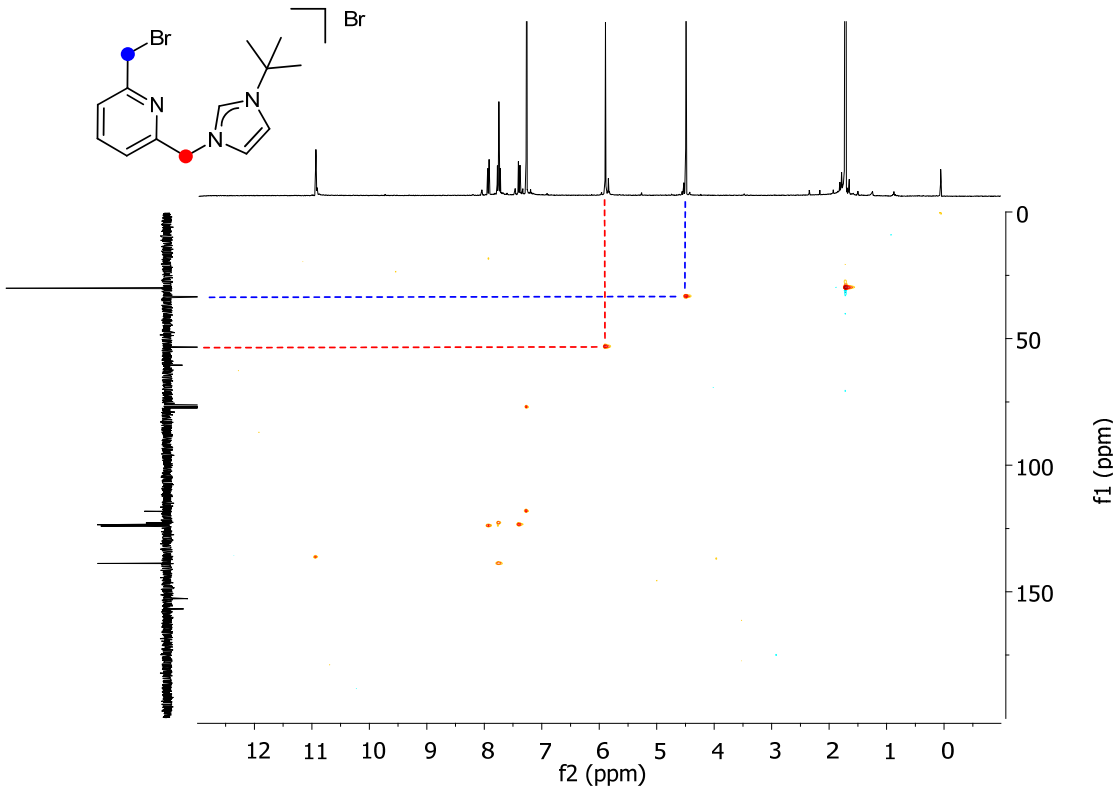

Figure S4. ^{1}H-^{13}C HSQC of [^{t}BuHImCH$_2$PyCH$_2$Br]Br (**1**) registered in CDCl$_3$.

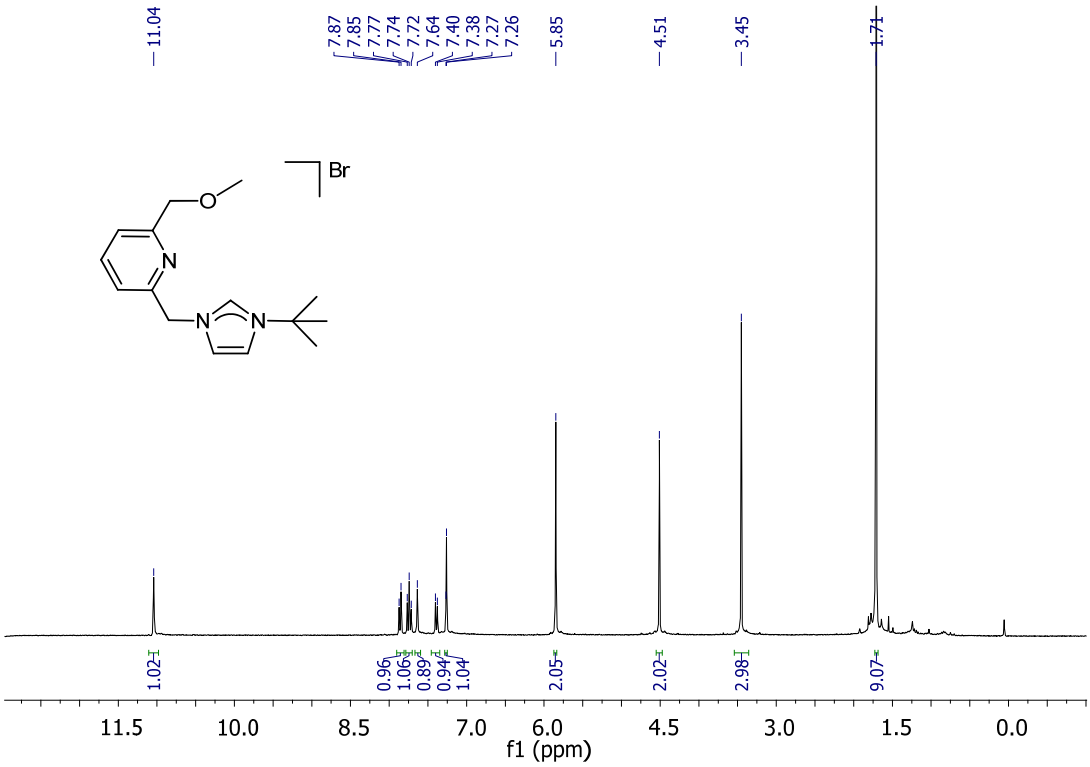

Figure S5. ^{1}H NMR of [^{t}BuHImCH$_2$PyCH$_2$OMe]Br (**2**) registered in CDCl$_3$.

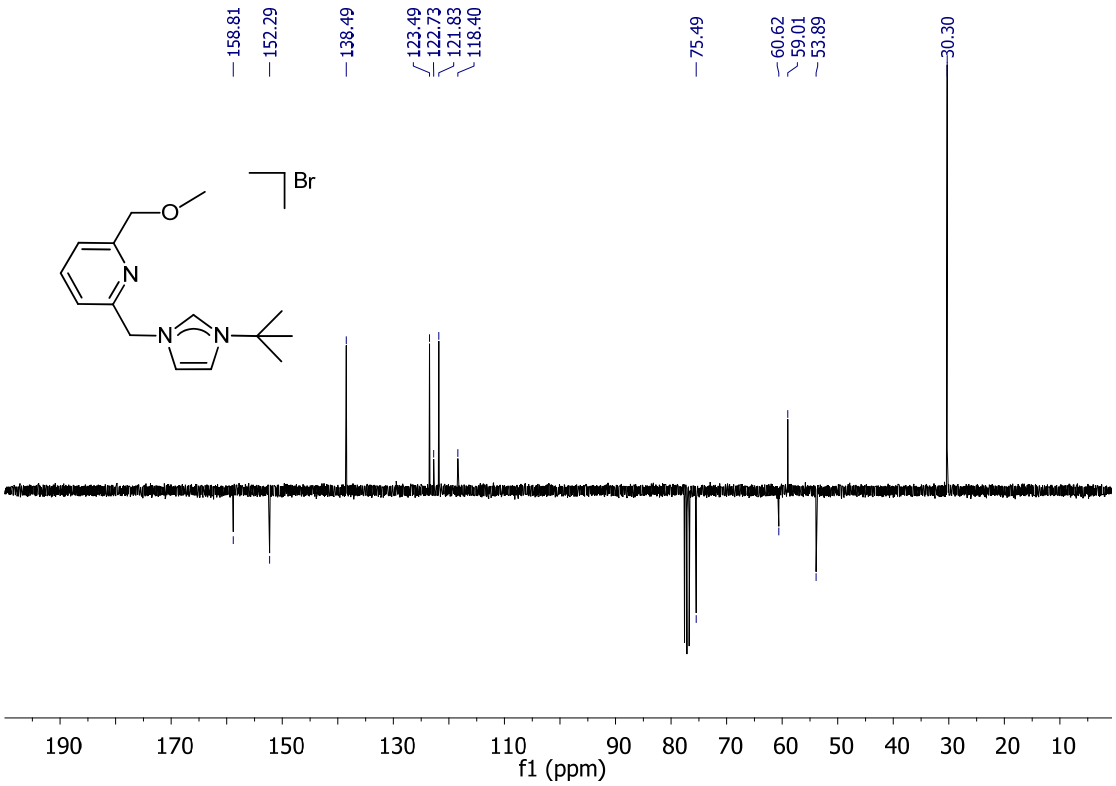

Figure S6. ^{13}C NMR APT of [^{t}BuHImCH$_2$PyCH$_2$OMe]Br (**2**) registered in CDCl$_3$.

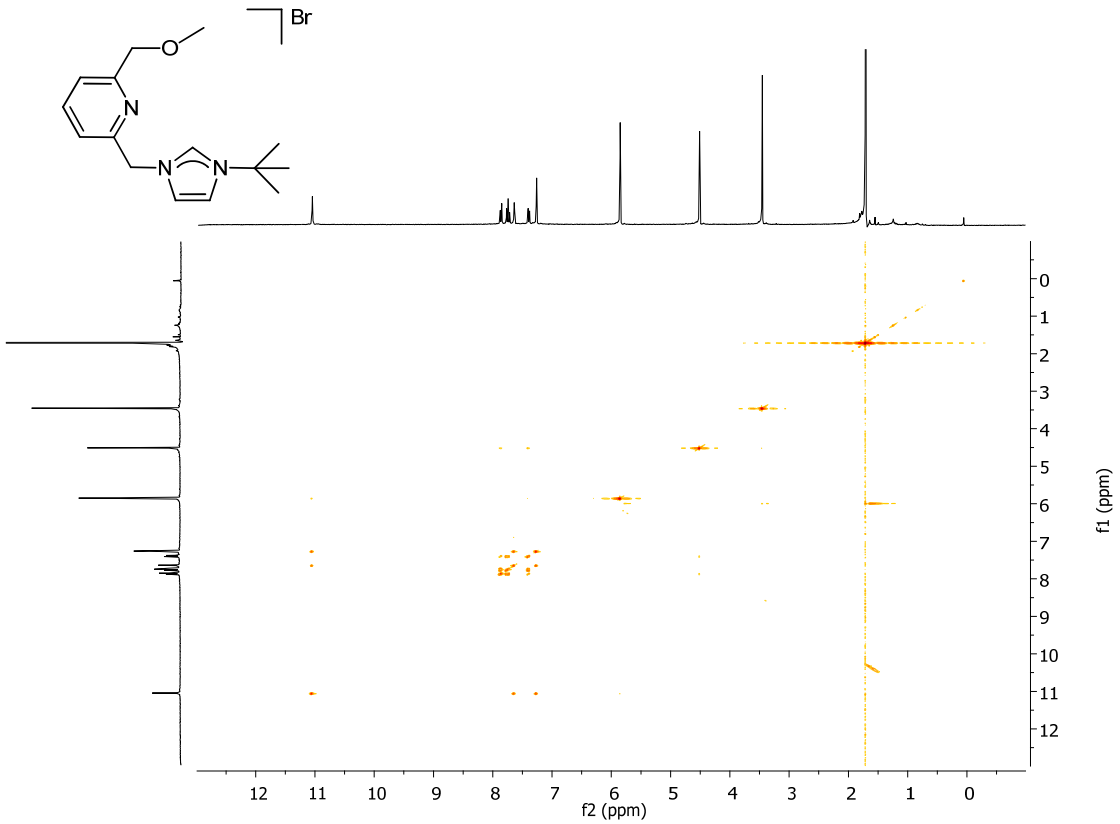

Figure S7. ^{1}H-^{1}H COSY of [^{t}BuHImCH$_2$PyCH$_2$OMe]Br (**2**) registered in CDCl$_3$.

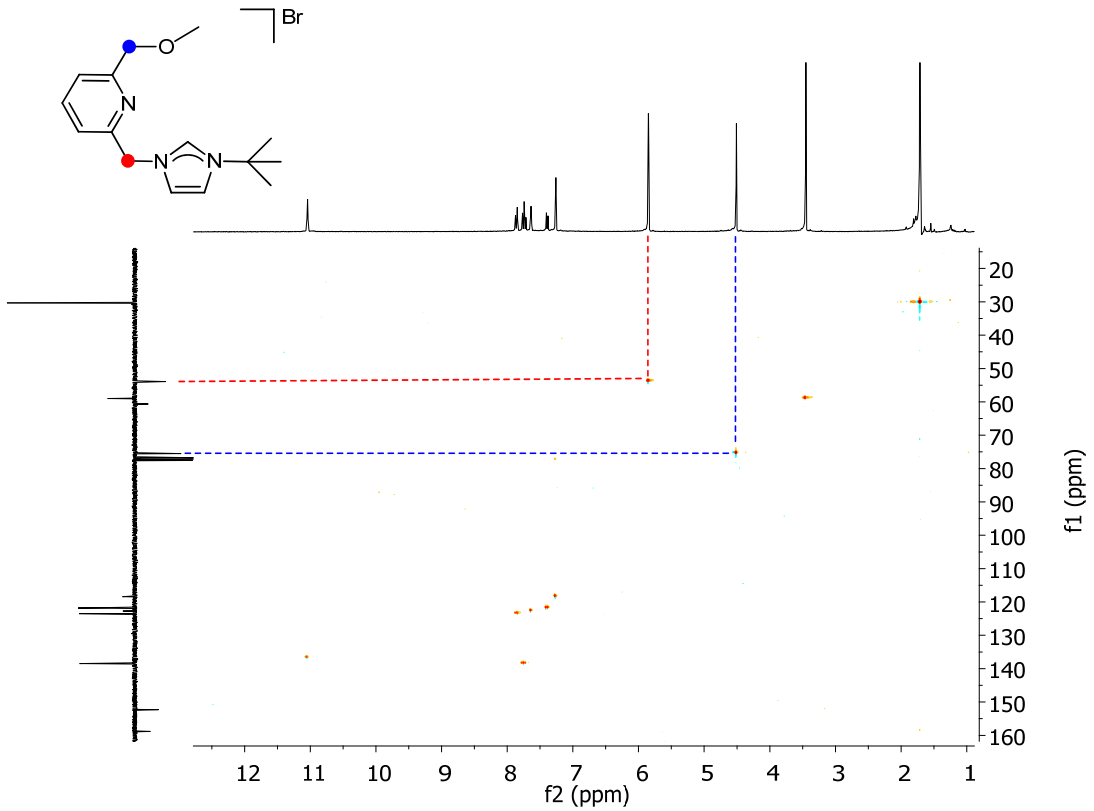

Figure S8. ^{1}H-^{13}C HSQC of [^{t}BuHImCH$_2$PyCH$_2$OMe]Br (**2**) registered in CDCl$_3$.

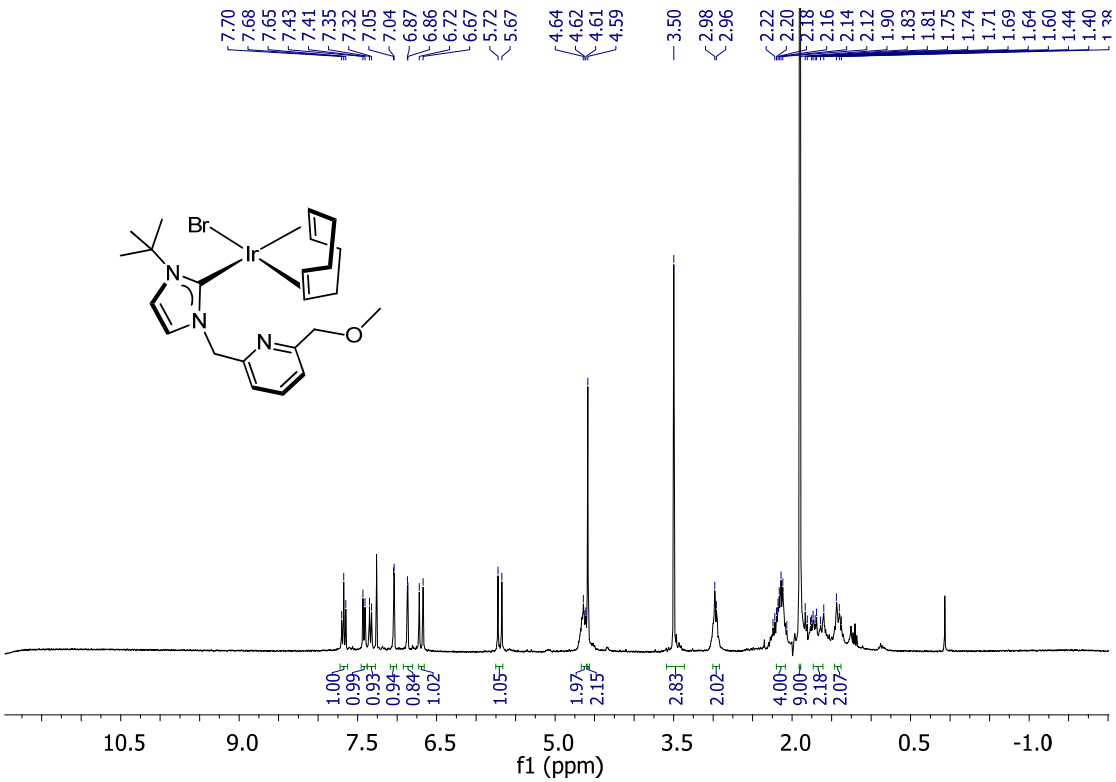

Figure S9. ^{1}H NMR of [IrBr(cod)(κ-*C*-^{t}BuImCH$_2$PyCH$_2$OMe)] (**3**) registered in $CDCl_3$.

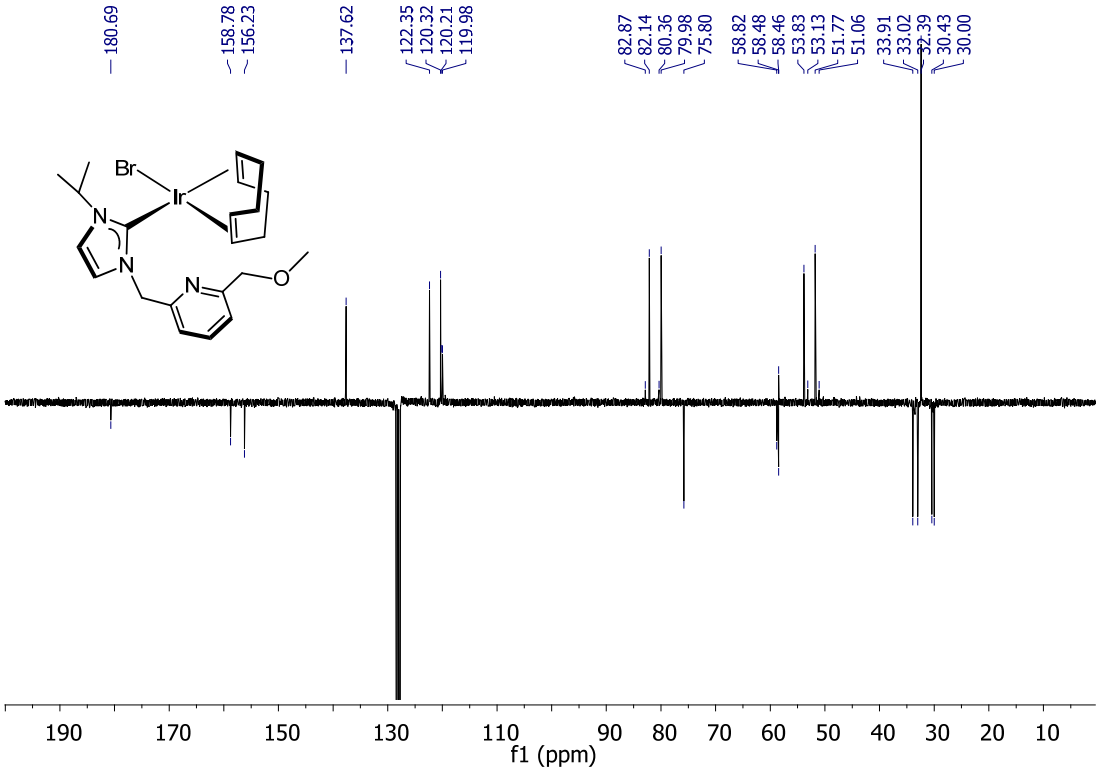

Figure S10. ^{13}C NMR APT of [IrBr(cod)(κ-*C*-^{t}BuImCH$_2$PyCH$_2$OMe)] (**3**) registered in C_6D_6.

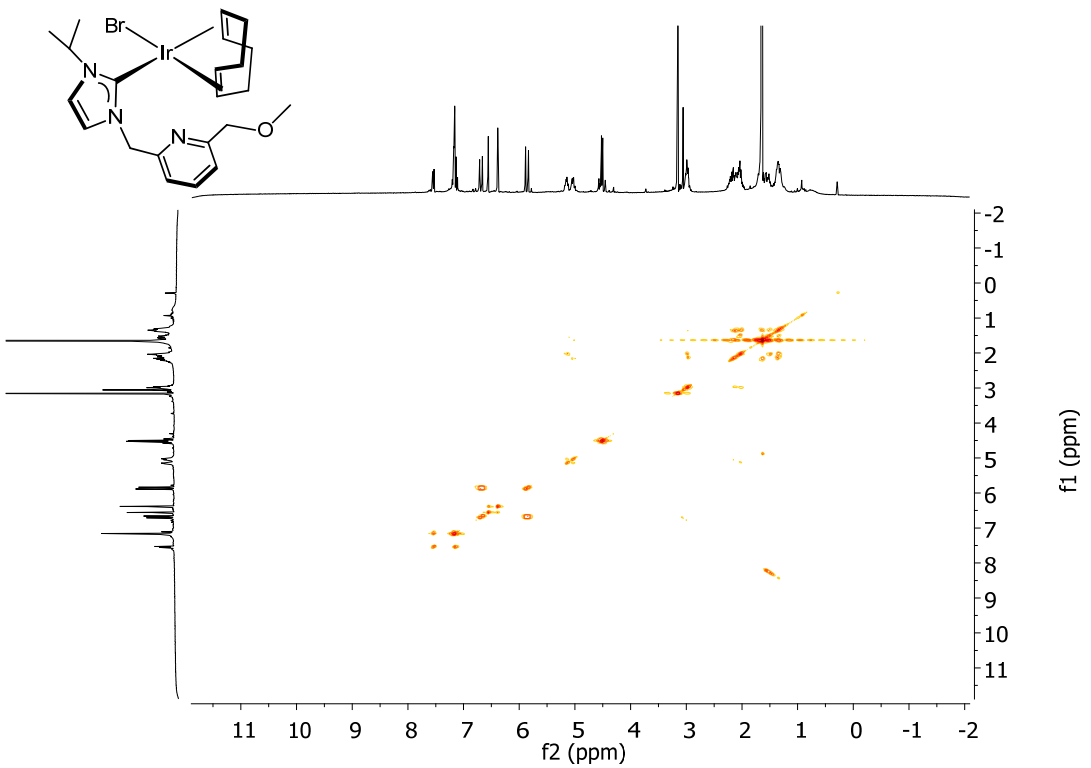

Figure S11. ^{1}H-^{1}H COSY of [IrBr(cod)(κ-*C*-^{t}BuImCH$_2$PyCH$_2$OMe)] (**3**) registered in $CDCl_3$.

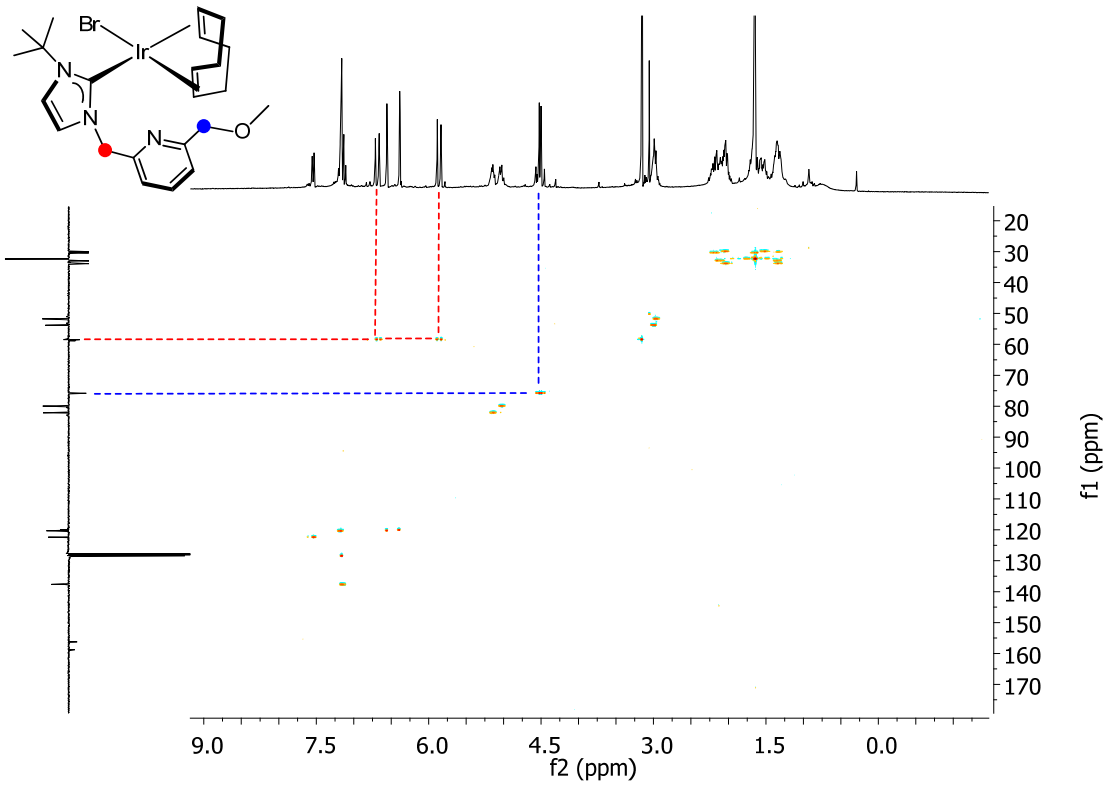

Figure S12. ^{1}H-^{13}C HSQC of [IrBr(cod)(κ-*C*-^{t}BuImCH$_2$PyCH$_2$OMe)] (**3**) registered in $CDCl_3$.

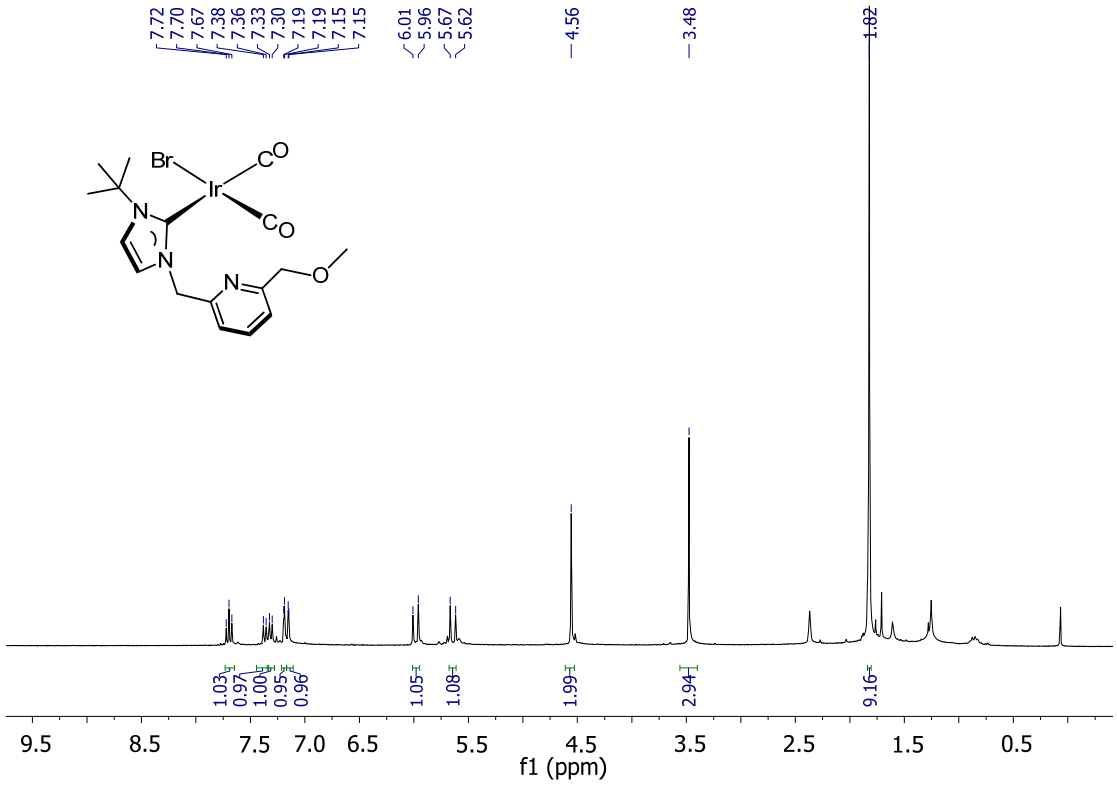

Figure S13. ^{1}H NMR of [IrBr(CO)$_2$(κ-*C*-^{t}BuImCH$_2$PyCH$_2$OMe)] (**4**) registered in CDCl$_3$.

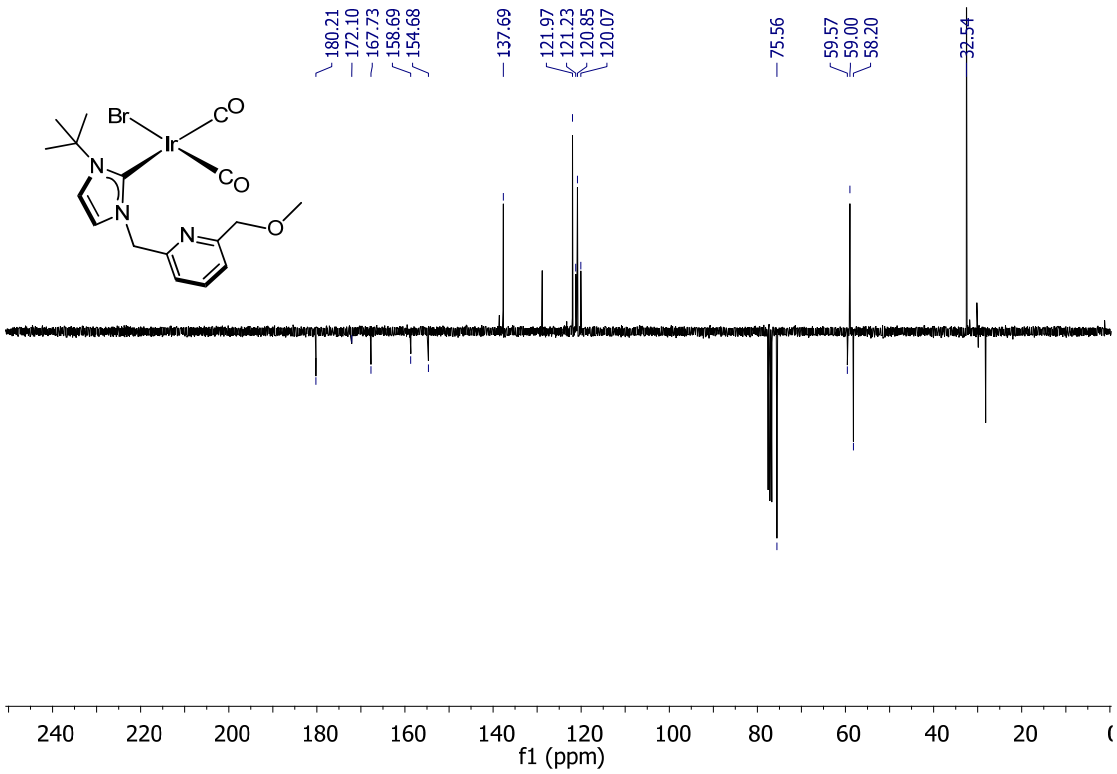

Figure S14. ^{13}C NMR APT of [IrBr(CO)$_2$(κ-*C*-^{t}BuImCH$_2$PyCH$_2$OMe)] (**4**) registered in CDCl$_3$.

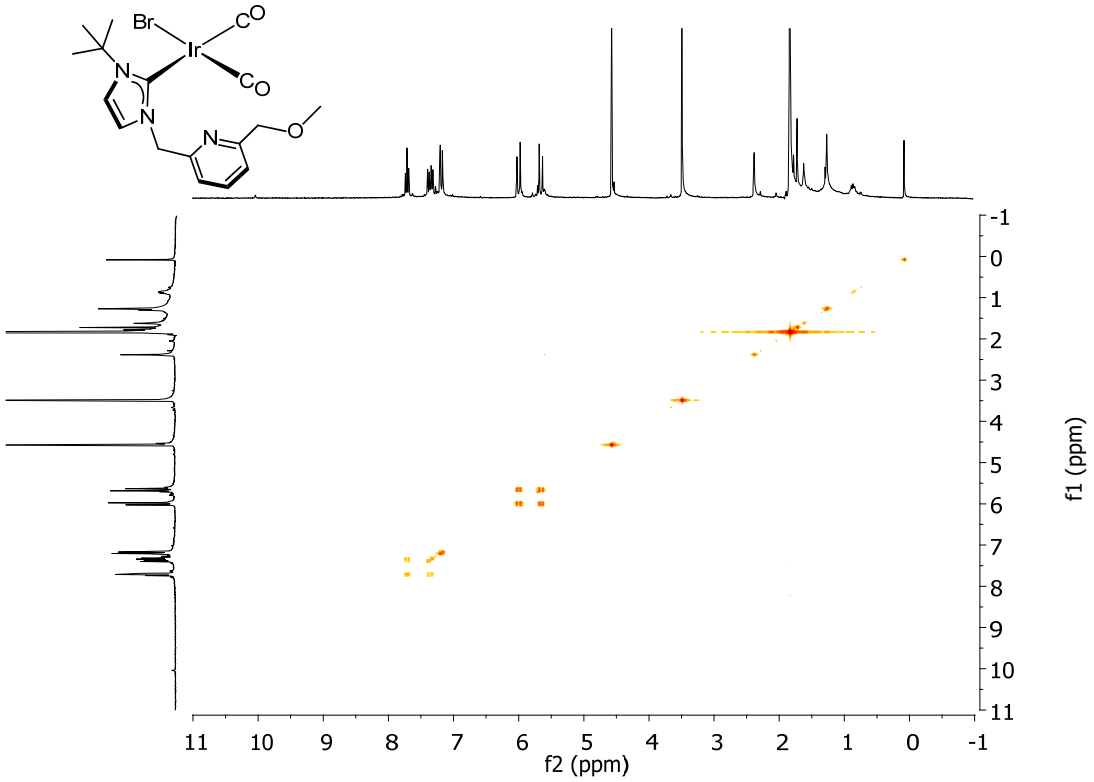

Figure S15. ^{1}H-^{1}H COSY of [IrBr(CO)$_2$(κ-*C*-^{t}BuImCH$_2$PyCH$_2$OMe)] (**4**) registered in CDCl$_3$.

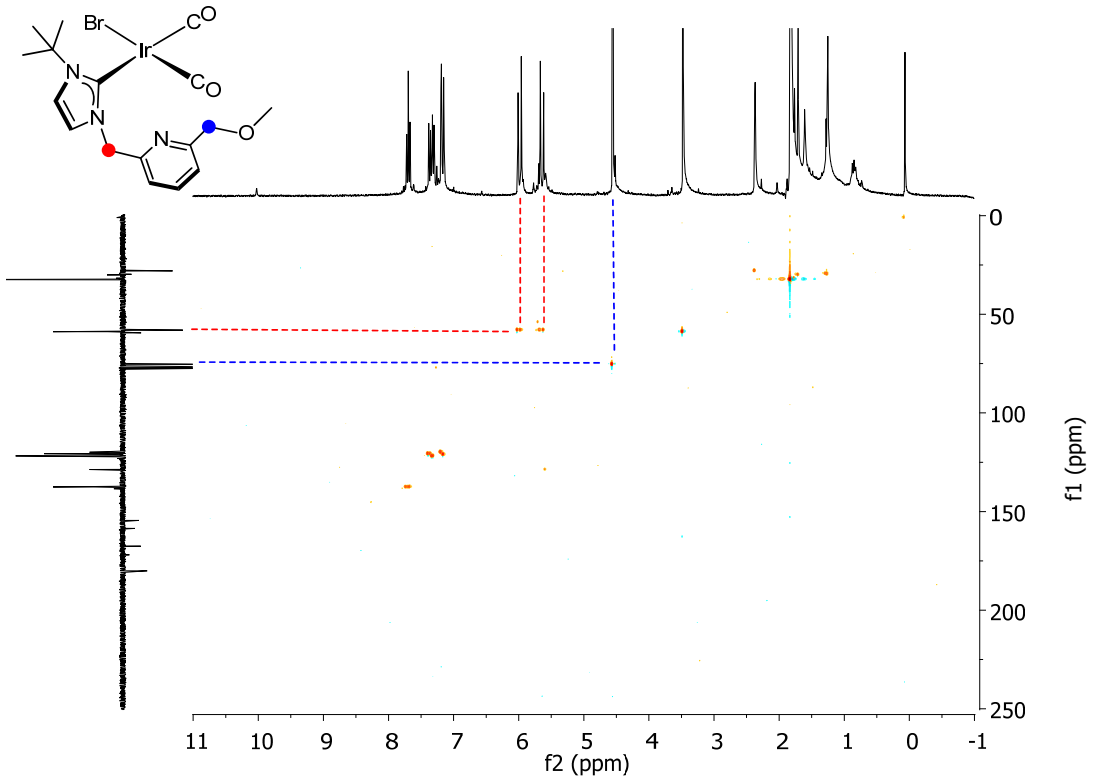

Figure S16. ^{1}H-^{13}C HSQC of [IrBr(CO)$_2$(κ-*C*-^{t}BuImCH$_2$PyCH$_2$OMe)] (**4**) registered in CDCl$_3$.

2.- Intermolecular contacts in the crystal structures of 3 and 4.

*2.1- Intermolecular contacts in the crystal structure of [IrBr(cod)(κC-^{t}BuImCH$_2$PyCH$_2$OMe)] (**3**).*[1]

Intermolecular contacts Br···H(15)' and H(27b)···C(14)" renders double chains growing along $\vec{b}$ (Figure S18).

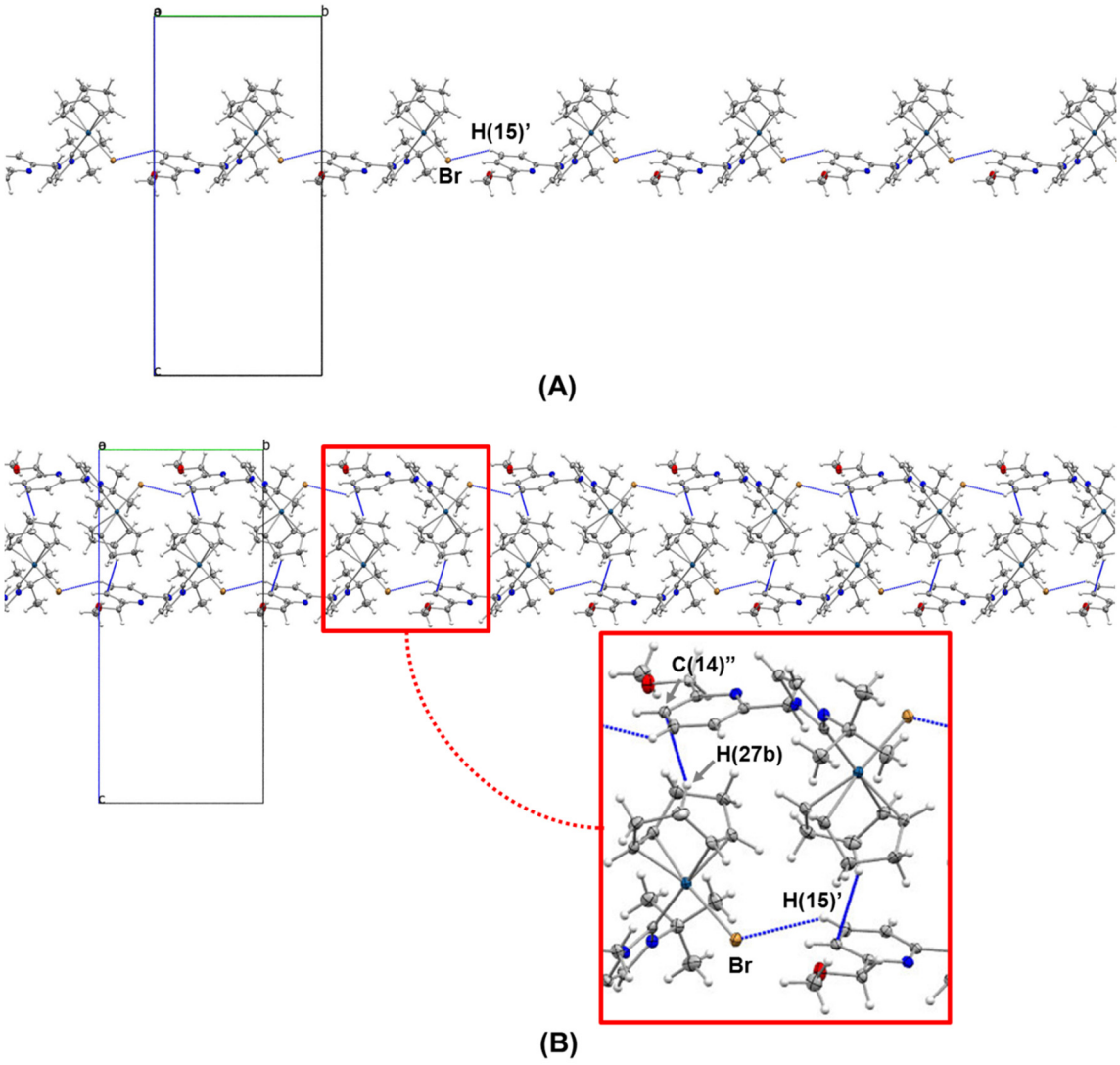

Figure S17. (A) View of the intermolecular contacts Br···H(15)' (2.9296(4) Å, equivalent positions: 1−x, 1/2+y, +1/2−z) rendering chains growing along $\vec{b}$. (B) View of the intermolecular contacts Br···H(15)' and C(14)"···H(27b) (2.7461(27) Å, equivalent positions: 1−x, 1/2+y, 1/2−z) rendering double chains growing along $\vec{b}$.

Adjacent double chains are joined by means of Br···H(4)' contacts (Figure S19-A) rendering the 2D array shown in Figure S19-B.

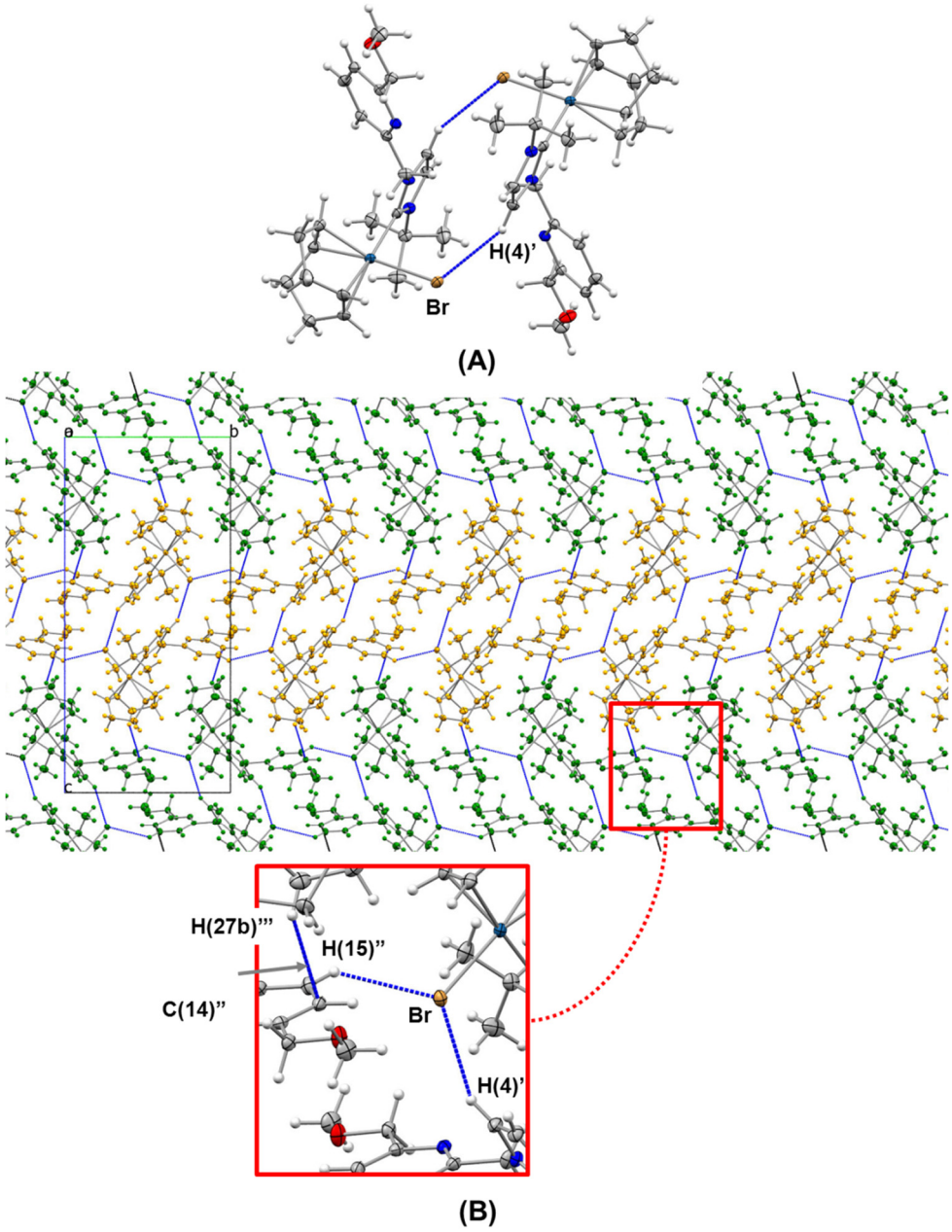

Figure S18. View of (A) the intermolecular contacts H(4)'···Br (3.0027(4) Å, equivalent positions: –x, –y, –z) and (B) the 2D array resulting from the intermolecular contacts Br···H(15)'', C(14)''···H(27b)''' (cf. Figure S18) and H(4)···Br. For clarity, i) green chains and orange chains are supported by Br···H(15)''; ii) pairing between adjacent green chains and between adjacent orange chains are supported by the Br···H(4)' contacts; and iii) pairing between adjacent orange and green chains are supported by the C(14)''···H(27b)''' contacts.

*2.2- Intermolecular contacts in the crystal structure of [IrBr(CO)$_2$(κC-^{t}BuImCH$_2$PyCH$_2$OMe)] (**4**).*[1]

Intermolecular contacts O(18)···H(3) and Br···H(14) result in the formation of chains growing along $\vec{b}$ and $\vec{a} + \vec{b}$, respectively (Figure S20). Figure S21 shows the resulting 2D array.

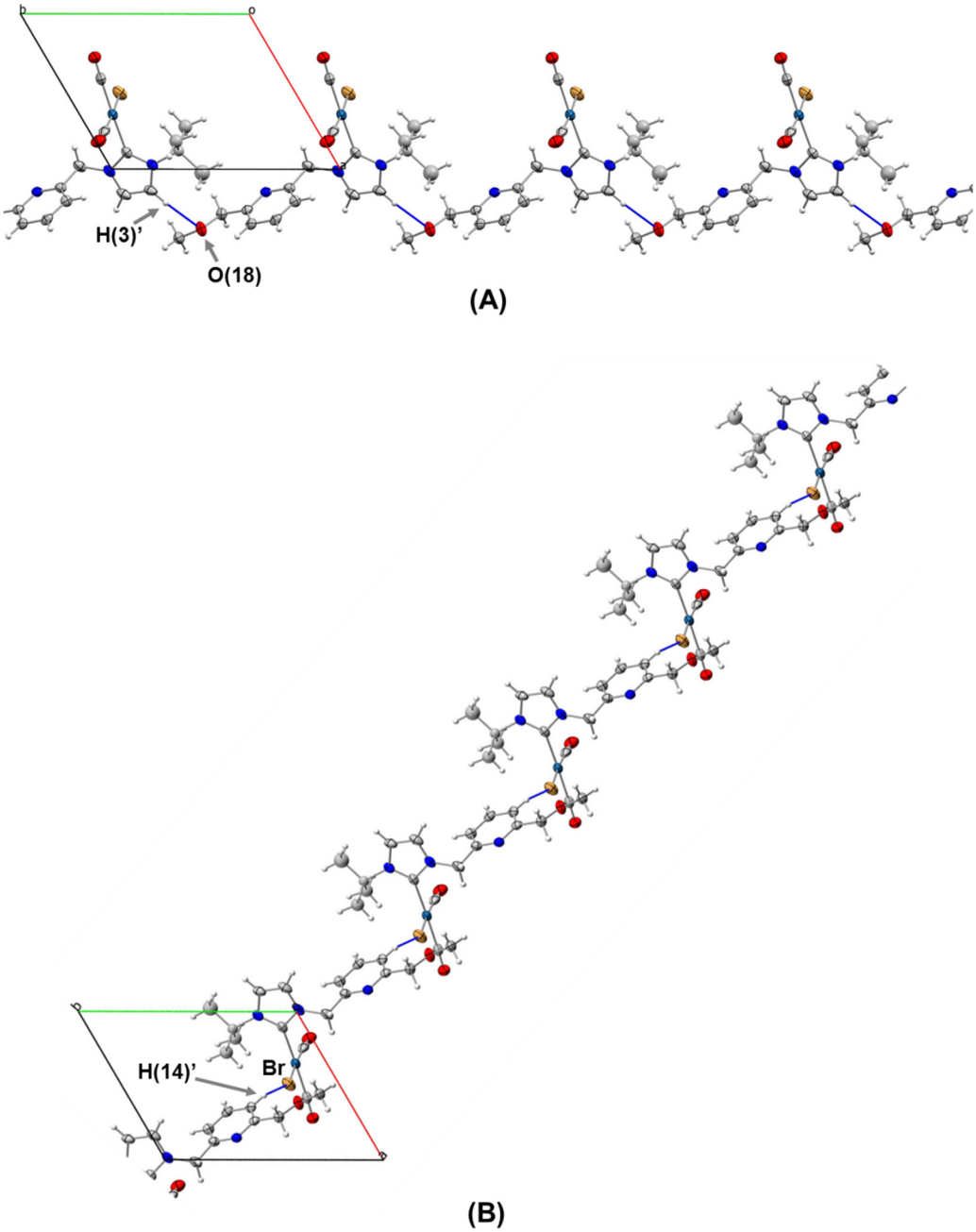

Figure S19. View of the intermolecular contacts (A) O(18)···H(3)' (2.533(5) Å, equivalent positions: x+1,+y+1,+z) and (B) Br···H(14)' (2.878(1) Å, equivalent positions: x+1,+y+1,+z) rendering chains growing along $\vec{b}$ and $\vec{a} + \vec{b}$, respectively.

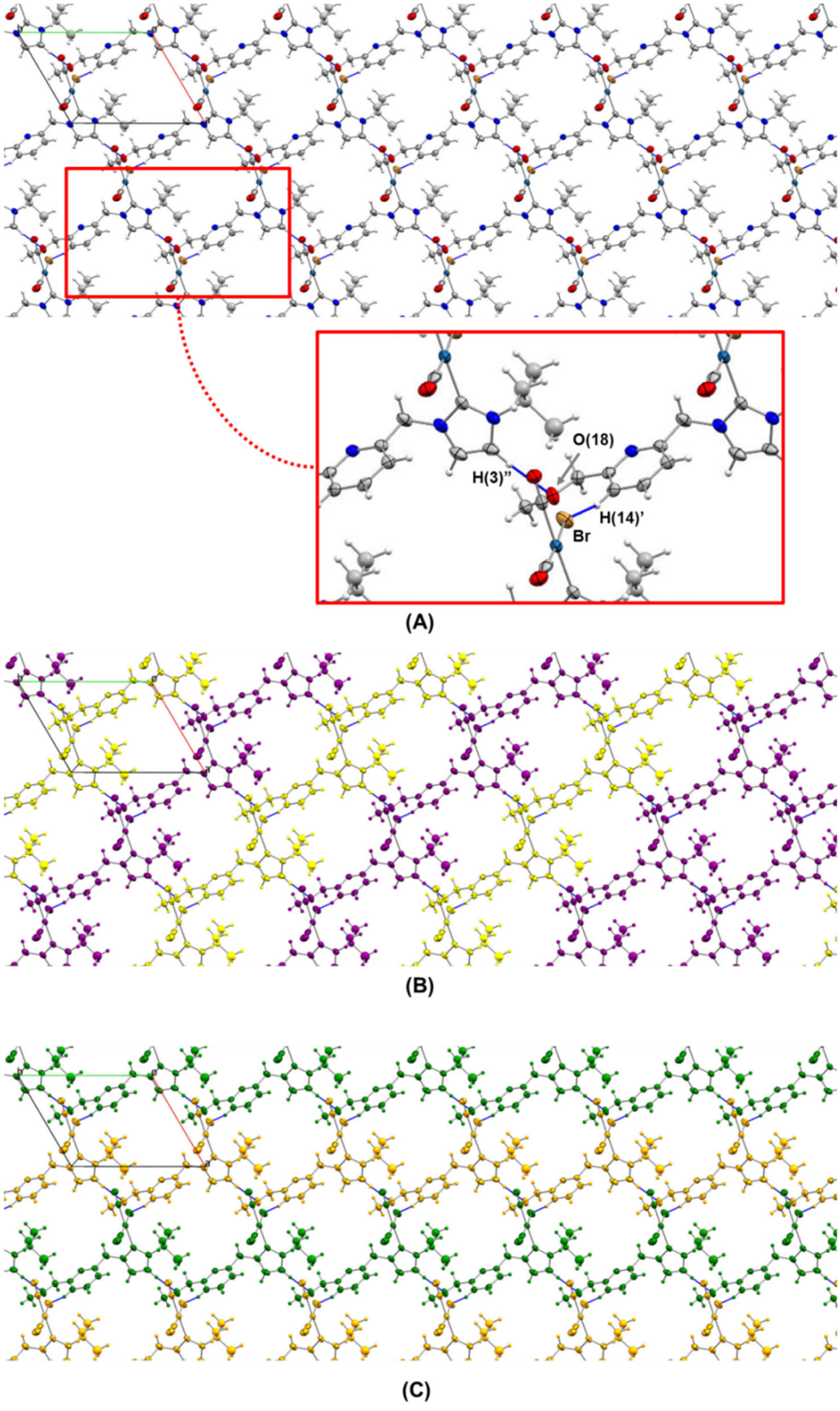

Figure S20. (A) View of the 2D array resulting from intermolecular contacts O(18)···H(3)' and Br···H(14)' (*cf.* Figure S20). (B) Adjacent chains supported by intermolecular contacts Br··· H(14)' are shown in yellow and purple. (C) Adjacent chains supported by intermolecular contacts O(18)···H(3) are shown in green and orange.

Also O(21)···H(19c) intermolecular contacts renders chains growing parallel to $\vec{b} + \vec{c}$ yielding the overall 3D packing of the asymmetric unit.

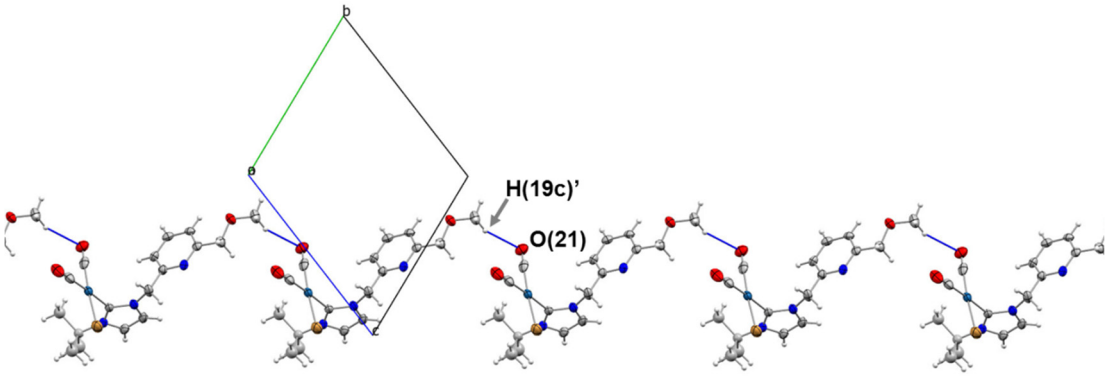

Figure S21. View of the intermolecular contacts O(21)···H(19c) (2.618(4) Å, equivalent positions: x+1,+y+1,+z+1) rendering chains growing along $\vec{b} + \vec{c}$.

It is worth a mention that additional intermolecular contacts are also present, namely H(4)···Br and O(21)···H(16) both rendering dimeric assemblies (Figure S23).

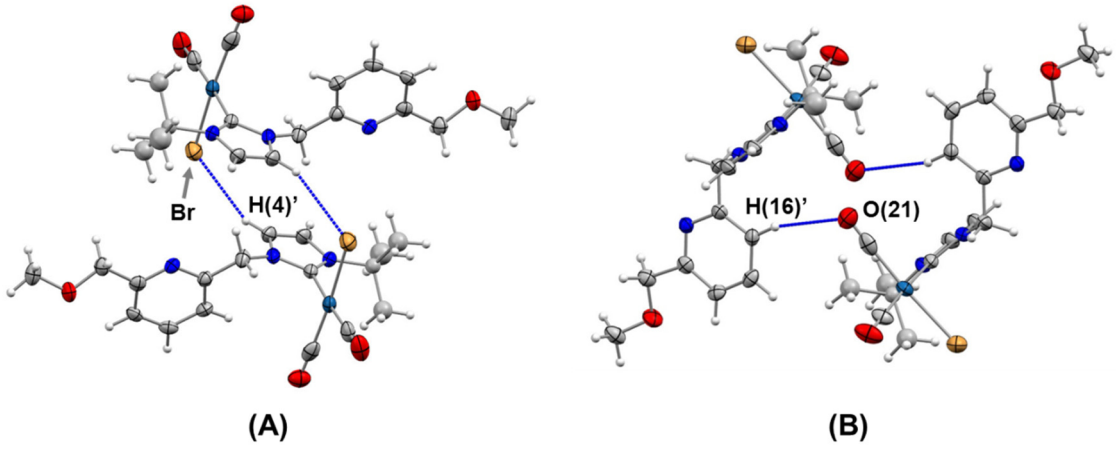

Figure S22. View of the dimers resulting from intermolecular contacts (A) Br···H(4)' (2.960(1) Å, equivalent positions: 2–x, –y, 2–z) and (B) O(21)···H(16)' (2.687(6) Å, equivalent positions: 2–x, –y, 1–z).

3.- Catalyst screening and optimization.

Table S1. Catalysts evaluation for the N-methylation of nitrobenzene with methanol.[a]

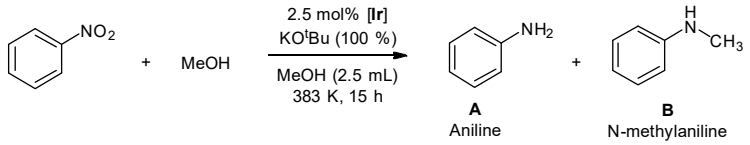

	Catalyst		Conversion (%)[b]	Selectivity (%)[b] A	B
1	-		-	-	-
2	[Ir(μ-Cl)(cod)]$_2$		100	73	27
3	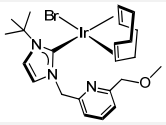	**3**	100	8	92
4	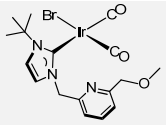	**4**	100	4	96

[a] Reaction conditions: nitrobenzene (0.5 mmol), catalyst (0.125 mmol, 2.5 mol%) and KO^{t}Bu (0.5 mmol, 100 mol%) in methanol (2.5 mL) at 383 K for 15 hours. [b] Conversion, based on the consumption of nitrobenzene, and selectivity determined by GC using mesitylene as internal standard.

Table S2. Influence of catalyst loading and temperature for the N-methylation of nitrobenzene with methanol catalyzed by [IrBr(CO)$_2$(κ-*C*-^{t}BuImCH$_2$PyCH$_2$OMe)] (**4**).[a]

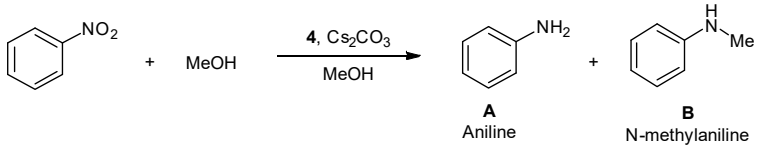

	T (K)	t (h)	4 (mol%)	Conversion (%)[b]	Selectivity (%)[b] A	B
1	403	24	0.5	100	0	100
2	333	24	2.5	100	57	43
3	333	48	2.5	100	14	86
4	333	24	1	100	71	29
5	333	48	1	100	26	74

[a] Reaction conditions: nitrobenzene (0.5 mmol, catalyst **4** (mol%), Cs_2CO_3 (0.375 mmol, 75 mol%) in methanol (2.5 mL). [b] Conversion, based on the consumption of nitrobenzene, and selectivity determined by GC using mesitylene as internal standard.

4.- Isotopic labeling experiments.

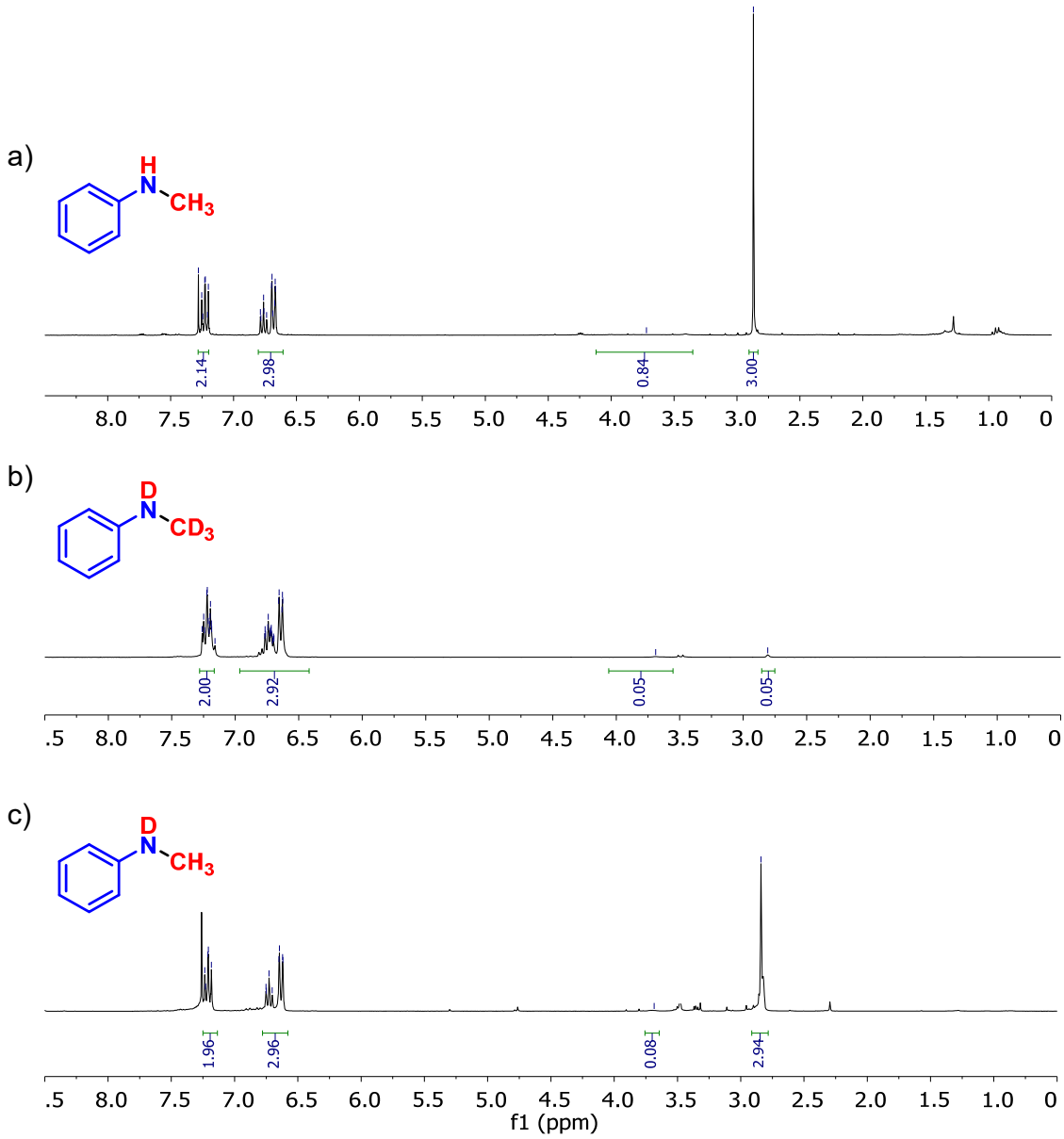

Figure S23. ^{1}H NMR ($CDCl_3$, 298 K): a) N-Methylaniline, b) N-Methylation of nitrobenzene with methanol-d_4, and c) N-Methylation of nitrobenzene with methanol-d_1.

5.- Isolation and characterization of N-methylated amines.

The reaction mixture obtained from catalytic reactions of N-methylation of nitroaromatic compounds, following the general procedure, was cooled to room temperature and then silica gel was added. The mixture was dried under vacuum and the residue transferred to a silica gel column and then eluted using the corresponding eluent described for each product.

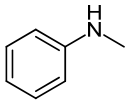

N-methylaniline.[2] Nitrobenzene (0.5 mmol, 51 μL). Purification by column chromatography (AcOEt/petroleum ether 15:85) obtaining 49 mg (92%) as a yellow oil. ^{1}H NMR (298 K, 300 MHz, $CDCl_3$): δ 7.30–7.18 (m, 2H), 6.80–6.64 (m, 3H), 3.72 (br, 1H), 2.87 (s, 3H). $^{13}C\{^{1}H\}$ NMR (298 K, 75 MHz, $CDCl_3$): δ 149.0, 129.4, 117.9, 113.0, 31.2.

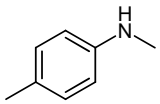

N,4-dimethylaniline.[2] 1-Methyl-4-nitrobenzene (0.5 mmol, 68 mg). Purification by column chromatography (AcOEt/petroleum ether 20:80) obtaining 59 mg (96%) as a yellow oil. ^{1}H NMR (298 K, 300 MHz, $CDCl_3$): δ 7.06–6.97 (m, 2H), 6.62–6.54 (m, 2H), 4.25 (br, 1H), 2.82 (s, 3H), 2.25 (s, 3H). $^{13}C\{^{1}H\}$ NMR (298 K, 75 MHz, $CDCl_3$): δ 146.9, 132.1, 129.1, 113.0, 31.4, 20.5.

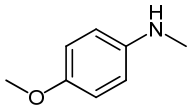

4-Methoxy-N-methylaniline.[2] 1-Methoxy-4-nitrobenzene (0.5 mmol, 76 mg). Purification by column chromatography (AcOEt/petroleum ether 30:70) obtaining 64 mg (93%) as a pale yellow solid. ^{1}H NMR (298 K, 300 MHz, $CDCl_3$): δ 6.84–6.77 (m, 2H), 6.65–6.59 (m, 2H), 3.76 (s, 3H), 3.65 (br, 1H), 2.81 (s, 3H). $^{13}C\{^{1}H\}$ NMR (298 K, 75 MHz, $CDCl_3$): δ 152.4, 143.4, 115.0, 114.0, 55.9, 31.9.

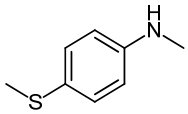

N-methyl-4-(methylthio)aniline.[3] 4-Nitrothioanisole (0.5 mmol, 84 mg). Purification by column chromatography (AcOEt/petroleum ether 10:90) obtaining 72 mg (94%) as a pale yellow oil. ^{1}H NMR (298 K, 300 MHz, $CDCl_3$): δ 7.30–7.22 (m, 2H), 6.65–6.58 (m, 2H), 3.96 (br, 1H), 2.85 (s, 3H), 2.43 (s, 3H). $^{13}C\{^{1}H\}$ NMR (298 K, 75 MHz, $CDCl_3$): δ 147.9, 131.6, 124.7, 113.4, 31.1, 19.3.

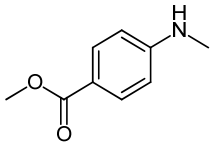

methyl 4-(methylamino)benzoate.[4] Methyl 4-nitrobenzoate (0.5 mmol, 91 mg). Purification by column chromatography (AcOEt/petroleum ether 20:80) obtaining 77 mg (93%) as a yellow oil. ^{1}H NMR (298 K, 300 MHz, $CDCl_3$): δ 7.93–7.84 (m, 2H), 6.67–6.57 (m, 2H), 4.71 (br, 1H), 3.85 (s, 3H), 2.89 (s, 3H). $^{13}C\{^{1}H\}$ NMR (298 K, 75 MHz, $CDCl_3$): δ 167.4, 152.3, 131.7, 119.1, 111.9, 51.7, 30.7.

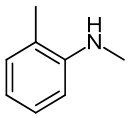

N,2-dimethylaniline.[4] 1-Methyl-2-nitrobenzene (0.5 mmol, 60 μL). Purification by column chromatography (AcOEt/petroleum ether 10:90) obtaining 52 mg (86%) as a colourless oil. ^{1}H NMR (298 K, 300 MHz, $CDCl_3$): δ 7.22–7.04 (m, 2H), 6.75–6.60 (m, 2H), 3.57 (br, 1H), 2.91 (s, 3H), 2.16 (s, 3H). $^{13}C\{^{1}H\}$ NMR (298 K, 75 MHz, $CDCl_3$): δ 147.1, 130.1, 127.3, 122.3, 117.8, 109.6, 31.1, 17.5.

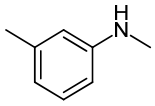

N,3-dimethylaniline.[5] 3-Methyl-2-nitrobenzene (0.5 mmol, 59 μL). Purification by column chromatography (AcOEt/petroleum ether 10:90) obtaining 48 mg (80%) as a yellow oil. ^{1}H NMR (298 K, 300 MHz, $CDCl_3$): δ 7.16–7.09 (m, 1H), 6.62–6.44 (m, 3H), 3.74 (br, 1H), 2.86 (s, 3H), 2.33 (s, 3H). $^{13}C\{^{1}H\}$ NMR (298 K, 75 MHz, $CDCl_3$): δ 149.4, 139.1, 129.2, 118.4, 113.4, 109.8, 31.0, 21.7.

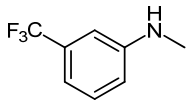

N-methyl-3-(trifluoromethyl)aniline.[3] 1-Nitro-3-(trifluoromethyl)benzene (0.5 mmol, 66 μL). Purification by column chromatography (AcOEt/petroleum ether 10:90) obtaining 79 mg (90%) as a colourless oil. ^{1}H NMR (298 K, 300 MHz, $CDCl_3$): δ 7.33–7.25 (m, 1H), 7.00–6.93 (m, 1H), 6.86–6.74 (m, 2H), 3.82 (br, 1H), 2.88 (s, 3H). $^{13}C\{^{1}H\}$ NMR (298 K, 75 MHz, $CDCl_3$): δ 149.3, 129.7, 126.3, 122.7, 115.8, 114.0, 108.8, 30.8.

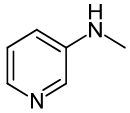

N-methylpyridin-3-amine.[2] 3-Nitropyridine (0.5 mmol, 62 mg). Purification by column chromatography (AcOEt) obtaining 43 mg (80%) as a pale yellow solid. ^{1}H NMR (298 K, 300 MHz, $CDCl_3$): δ 8.13–7.90 (m, 2H), 7.18–7.09 (m, 1H), 6.96–6.86 (m, 1H), 4.08 (br, 1H), 2.86 (s, 3H). $^{13}C\{^{1}H\}$ NMR (298 K, 75 MHz, $CDCl_3$): δ 152.6, 137.3, 134.9, 124.2, 118.7, 30.4.

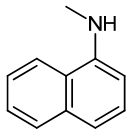

N-methylnaphthalen-1-amine.[2] 1-Nitronaphthalene (0.5 mmol, 86 mg). Purification by column chromatography (AcOEt/petroleum ether 25:75) obtaining 65 mg (82%) as a yellow oil. ^{1}H NMR (298 K, 300 MHz, $CDCl_3$): δ 7.88–7.77 (m, 2H), 7.53–7.26 (m, 4H), 6.69–6.61 (m, 1H), 4.50 (br, 1H), 3.04 (s, 3H). $^{13}C\{^{1}H\}$ NMR (298 K, 75 MHz, $CDCl_3$): δ 144.5, 134.3, 128.8, 126.8, 125.8, 124.8, 123.6, 119.9, 117.6, 104.1, 31.2.

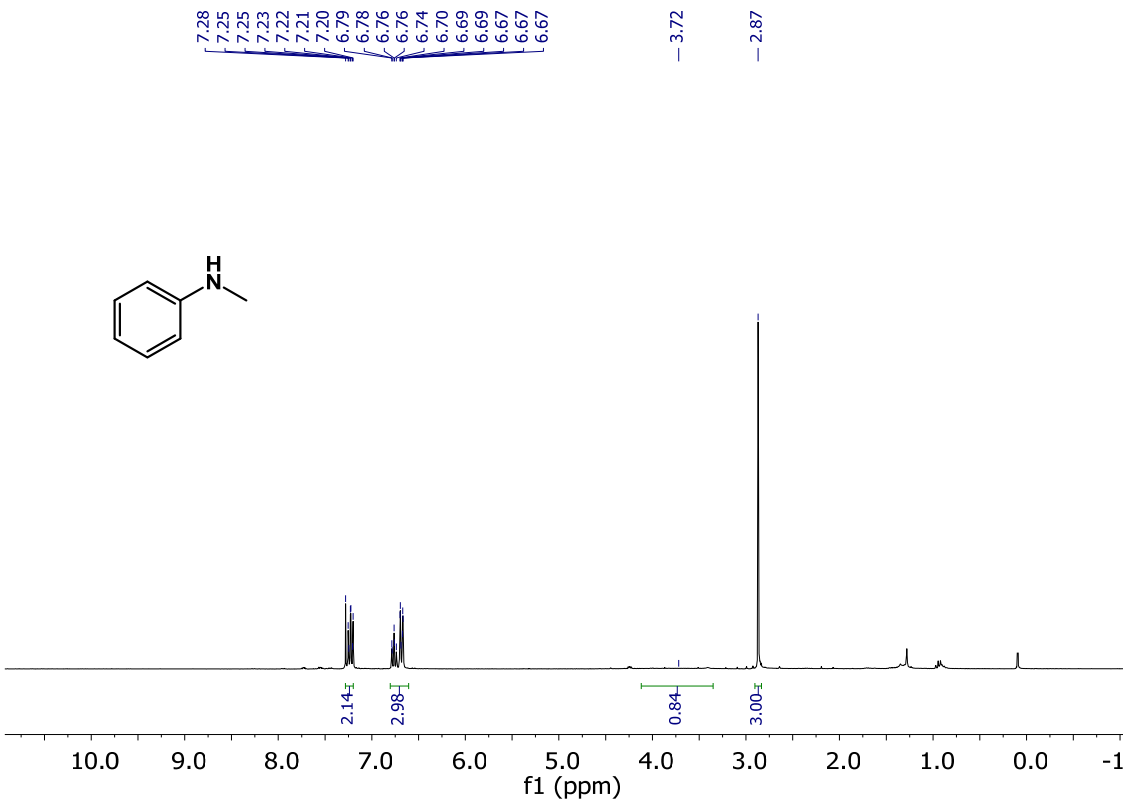

Figure S24. ^{1}H NMR of N-methylaniline.

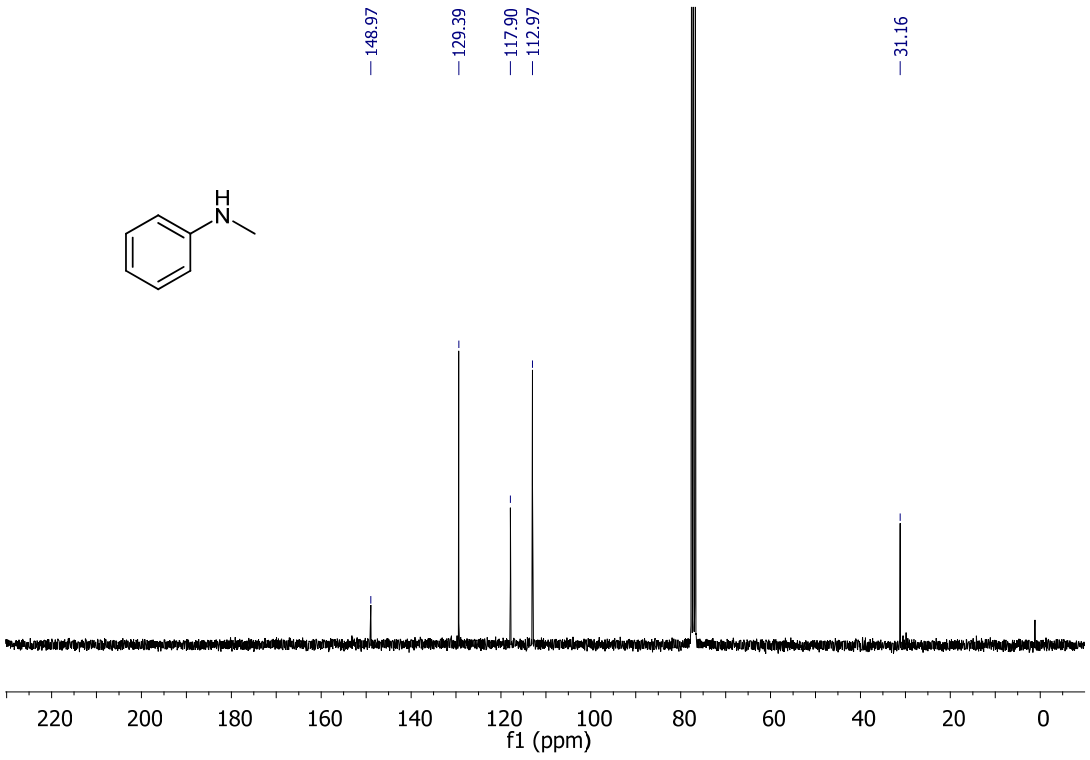

Figure S25. ^{13}C{^{1}H} NMR of N-methylaniline.

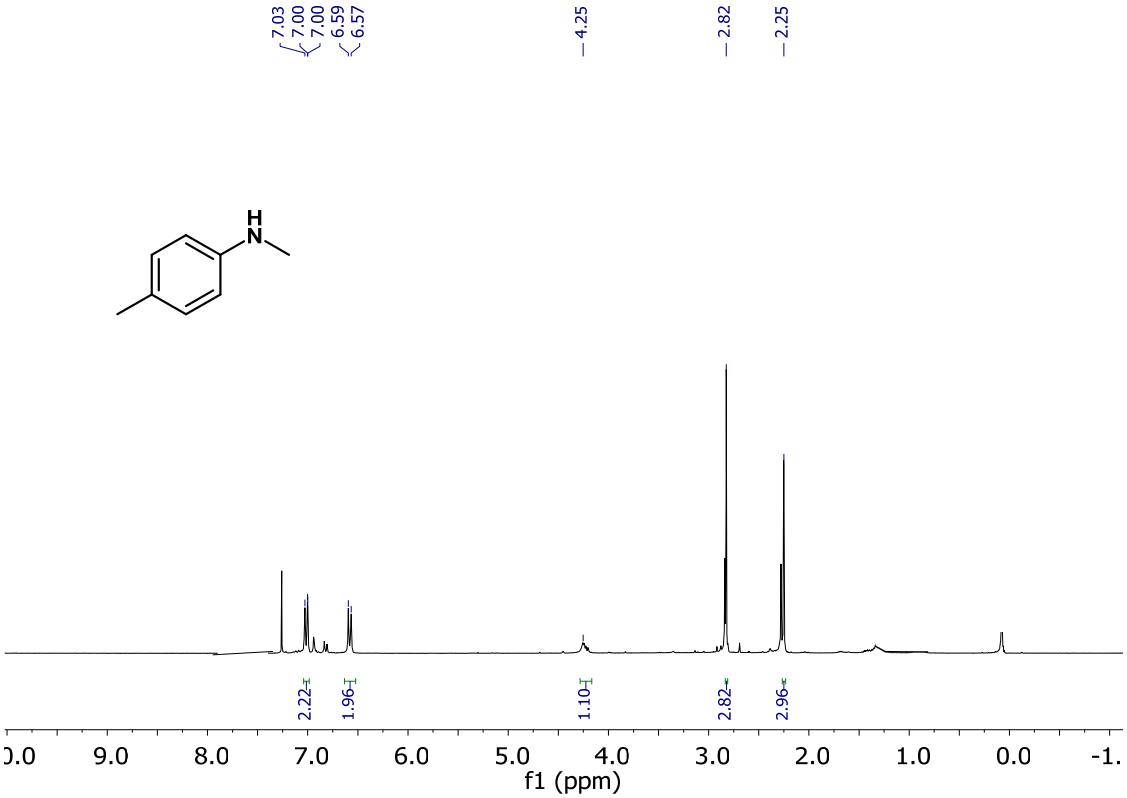

Figure S26. ^{1}H NMR of N,4-dimethylaniline.

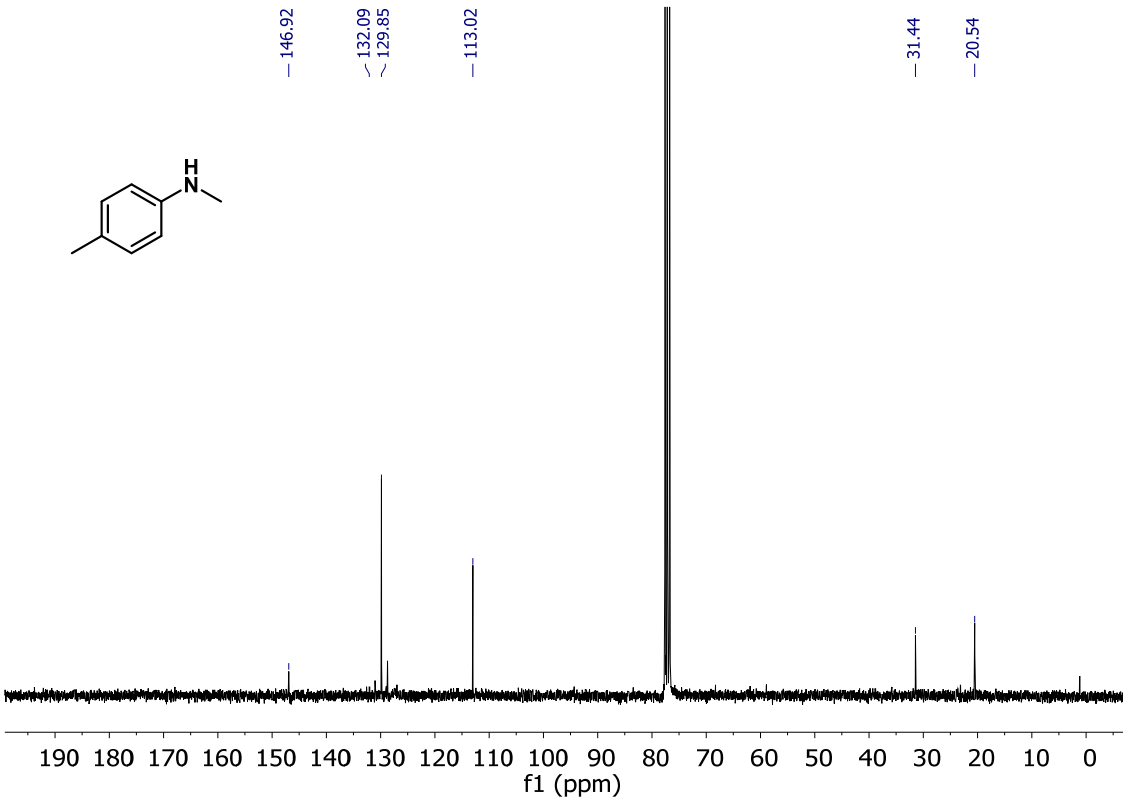

Figure S27. ^{13}C{^{1}H} NMR of N,4-dimethylaniline.

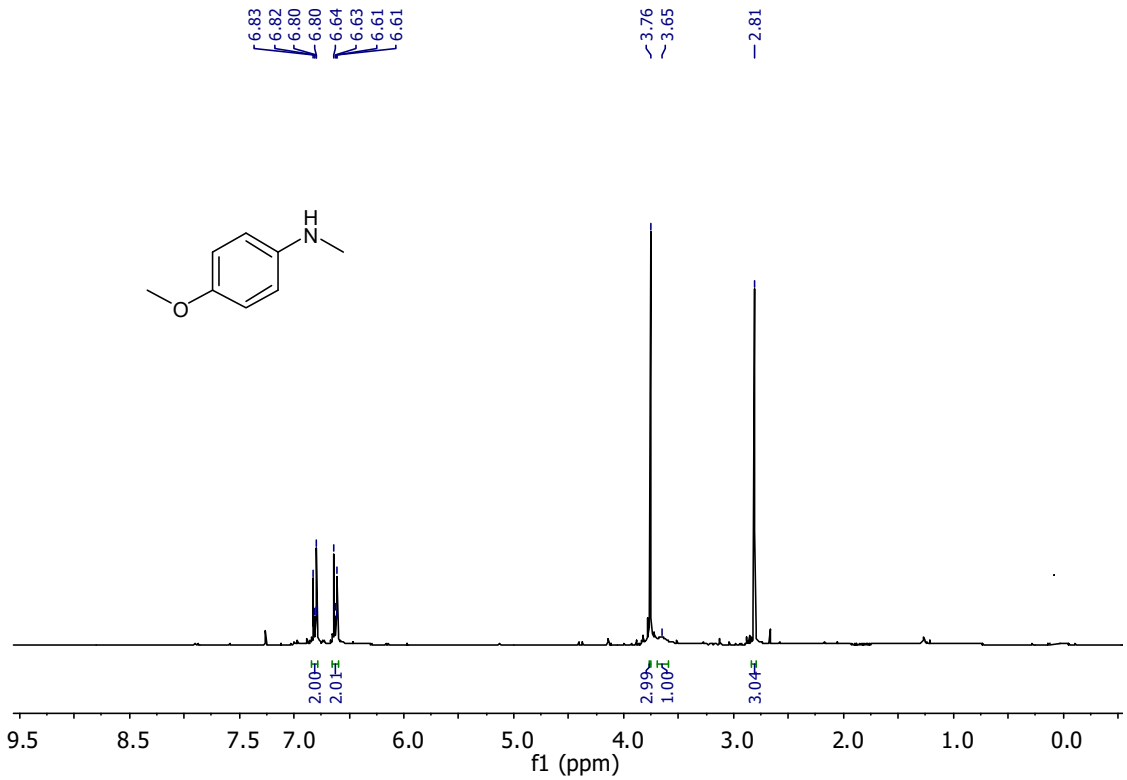

Figure S28. ^{1}H NMR of 4-methoxy-N-methylaniline.

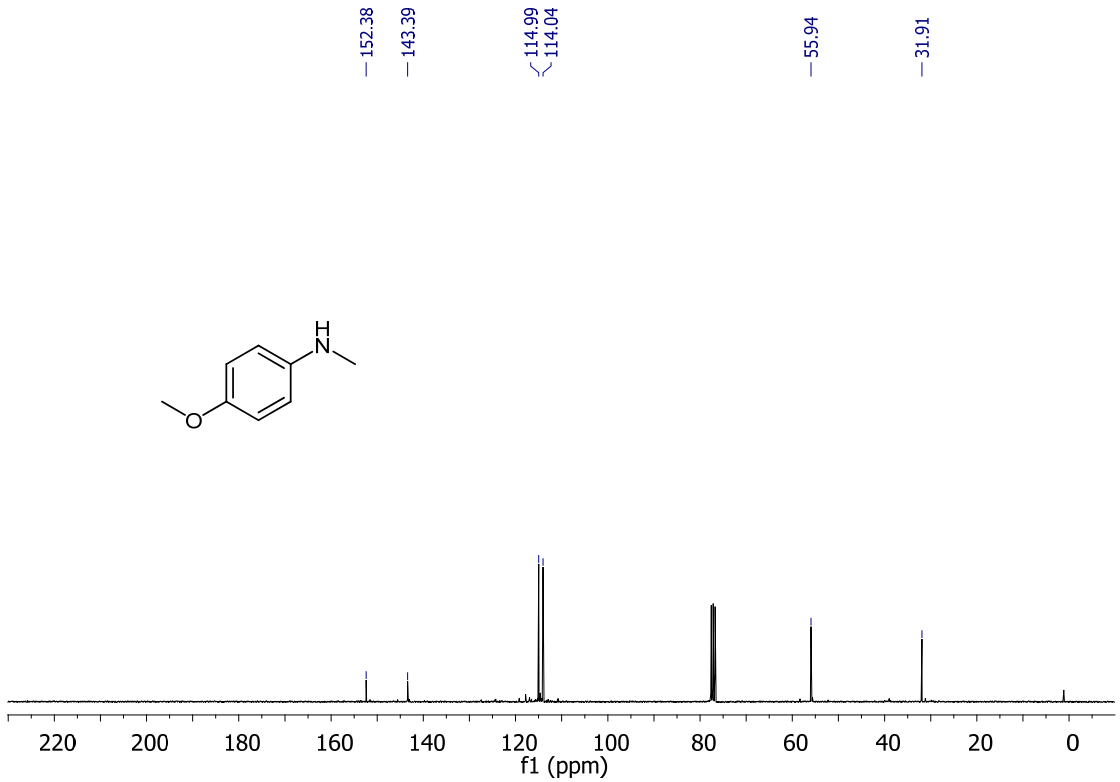

Figure S29. ^{13}C{^{1}H} NMR of 4-methoxy-N-methylaniline.

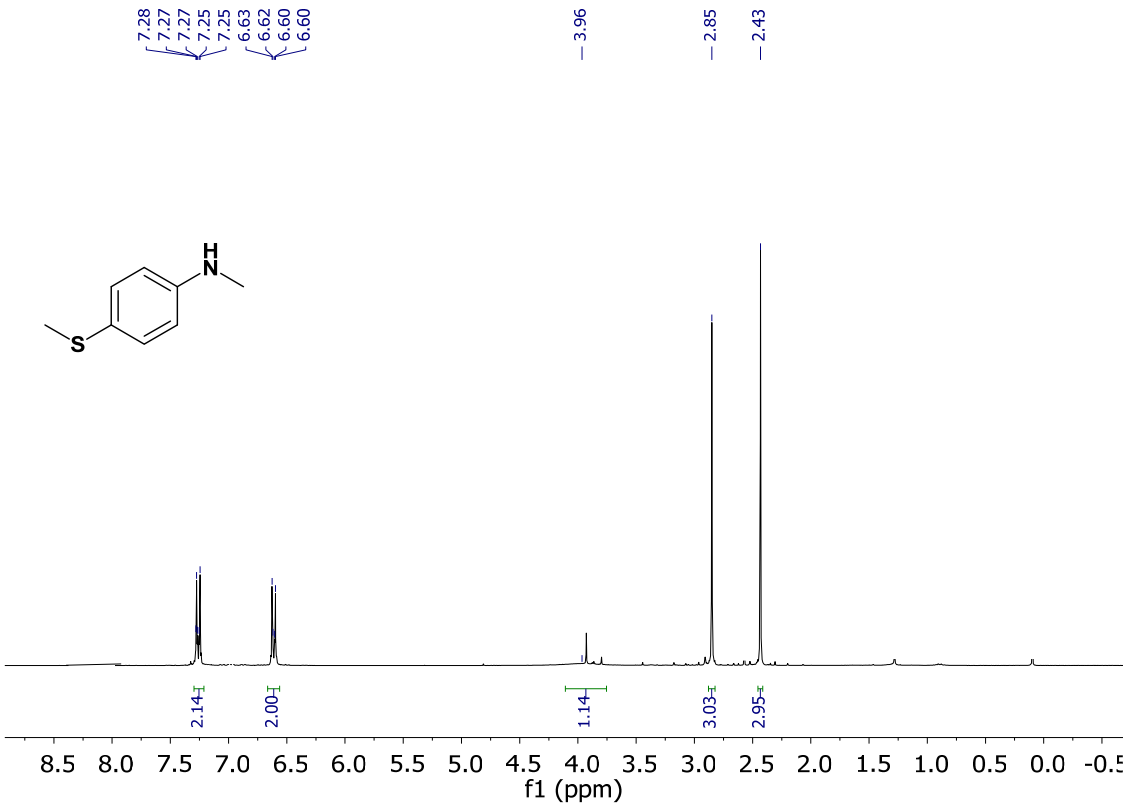

Figure S30. ^{1}H NMR of N-methyl-4-(methylthio)aniline.

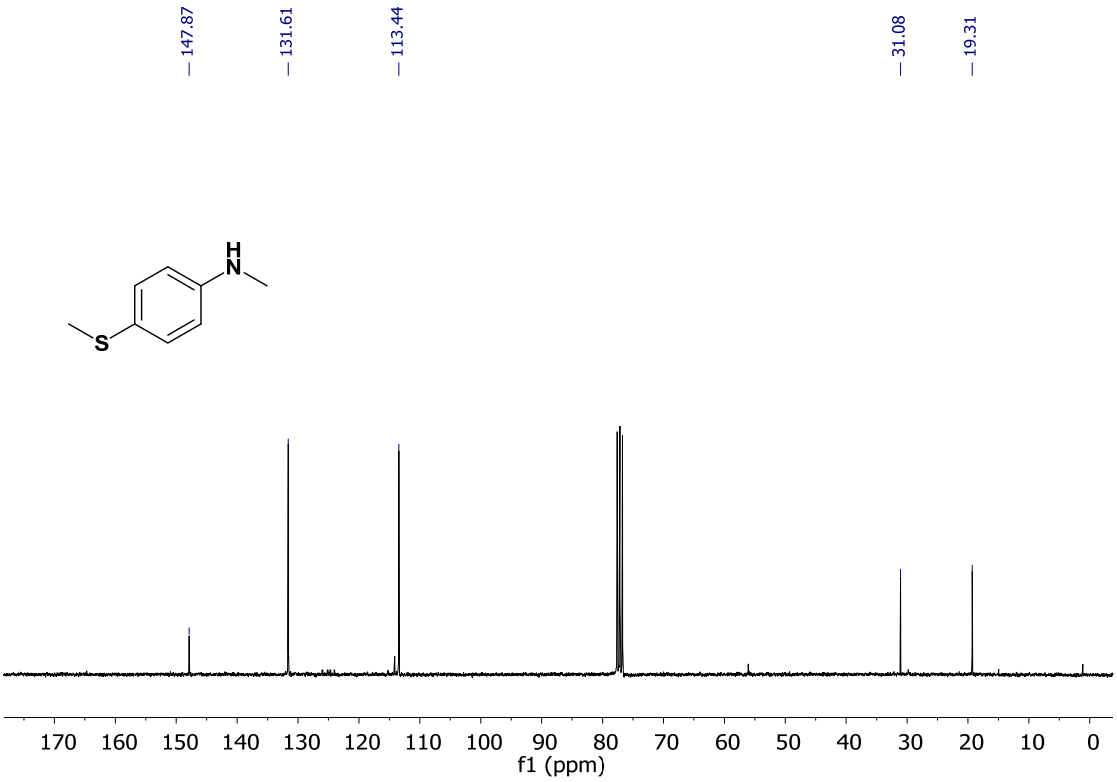

Figure S31. ^{13}C{^{1}H} NMR of N-methyl-4-(methylthio)aniline.

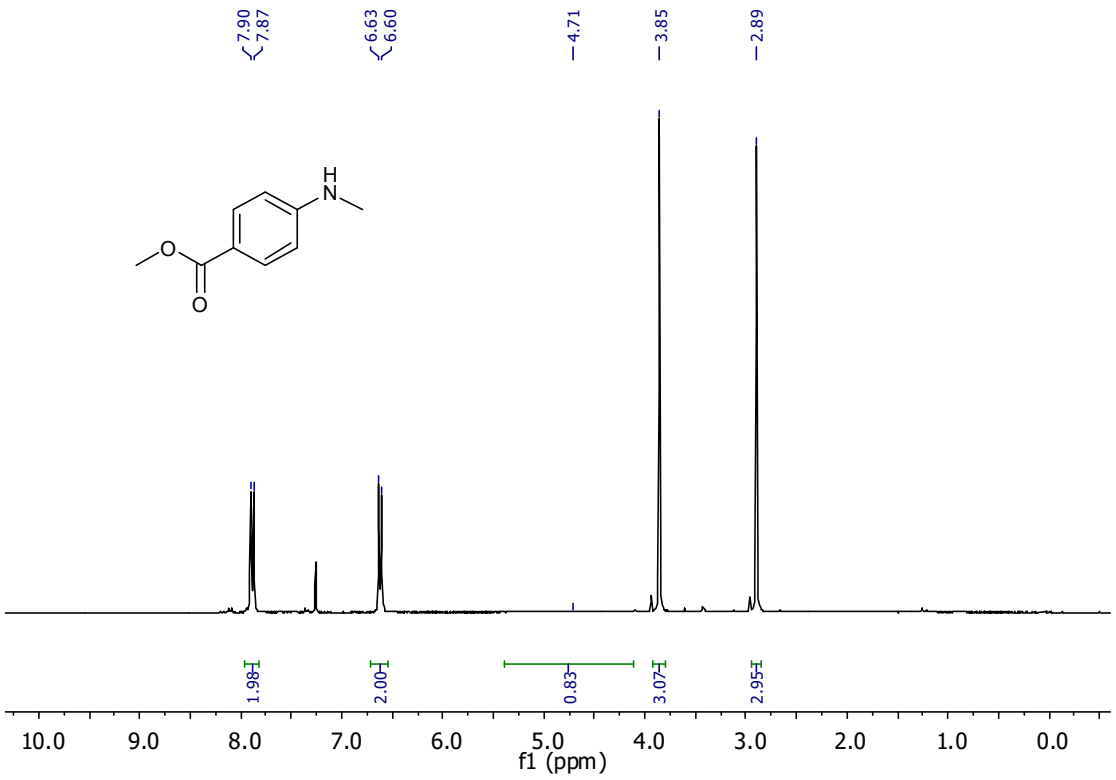

Figure S32. ^{1}H NMR of methyl 4-(methylamino)benzoate.

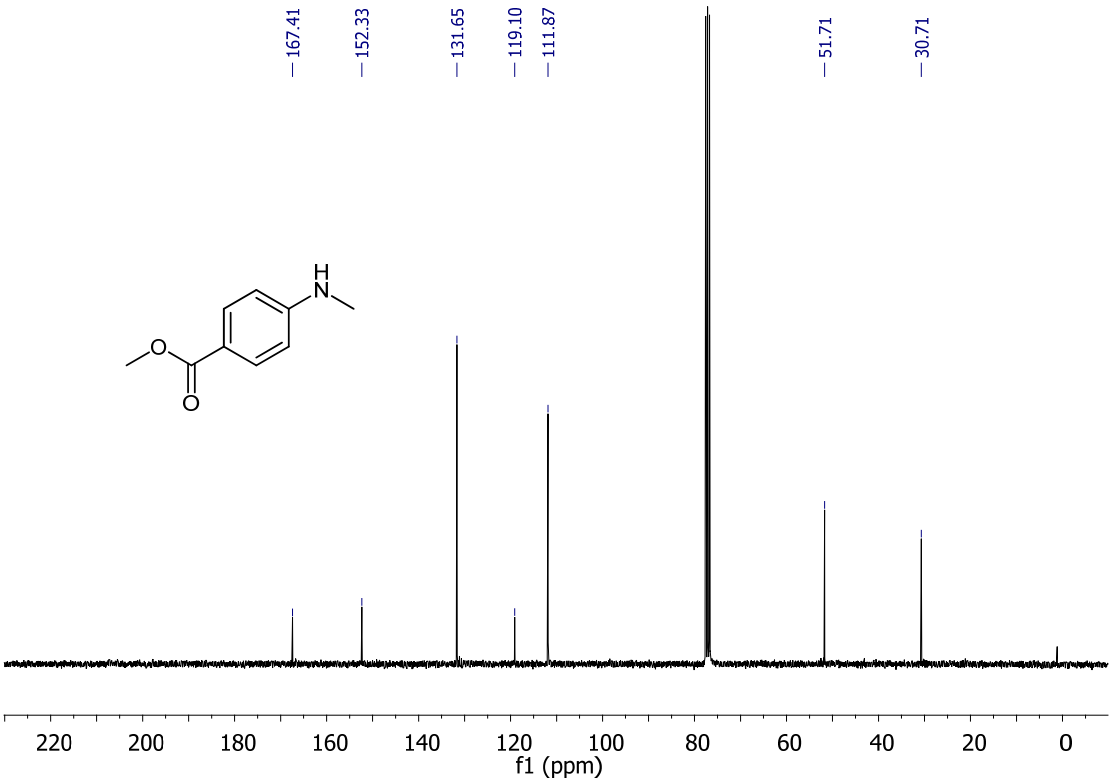

Figure S33. ^{13}C{^{1}H} of methyl 4-(methylamino)benzoate.

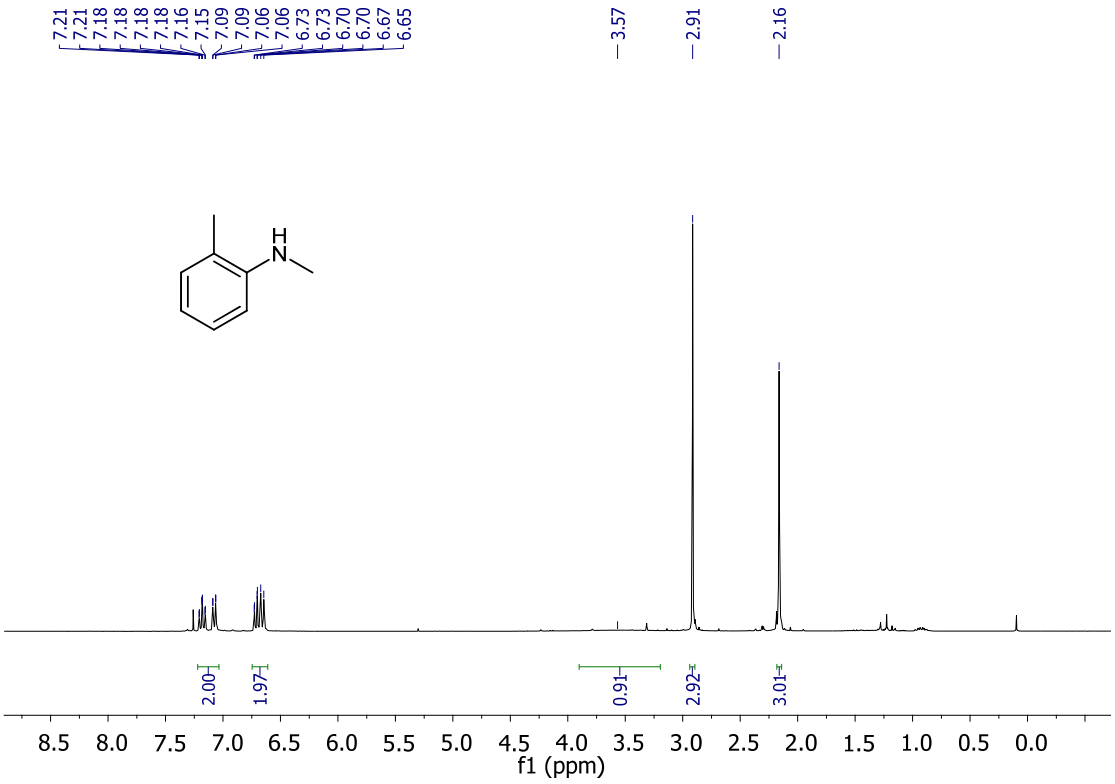

Figure S34. ^{1}H NMR of N,2-dimethylaniline.

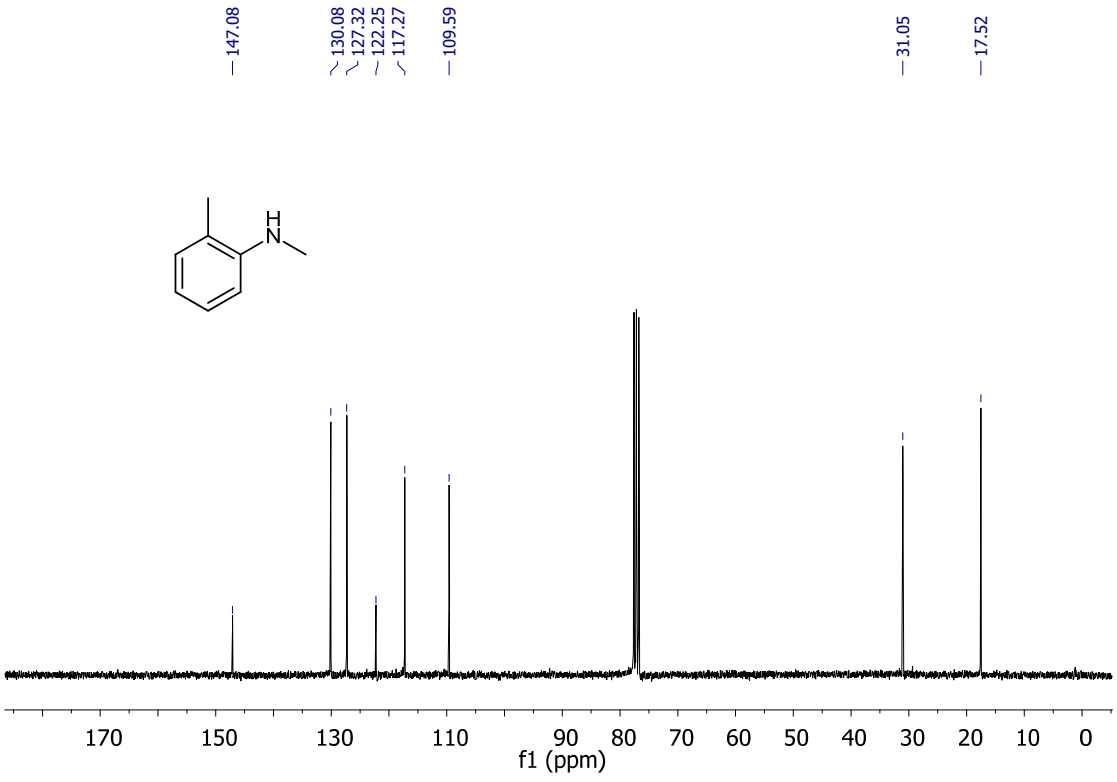

Figure S35. ^{13}C{^{1}H} NMR of N,2-dimethylaniline.

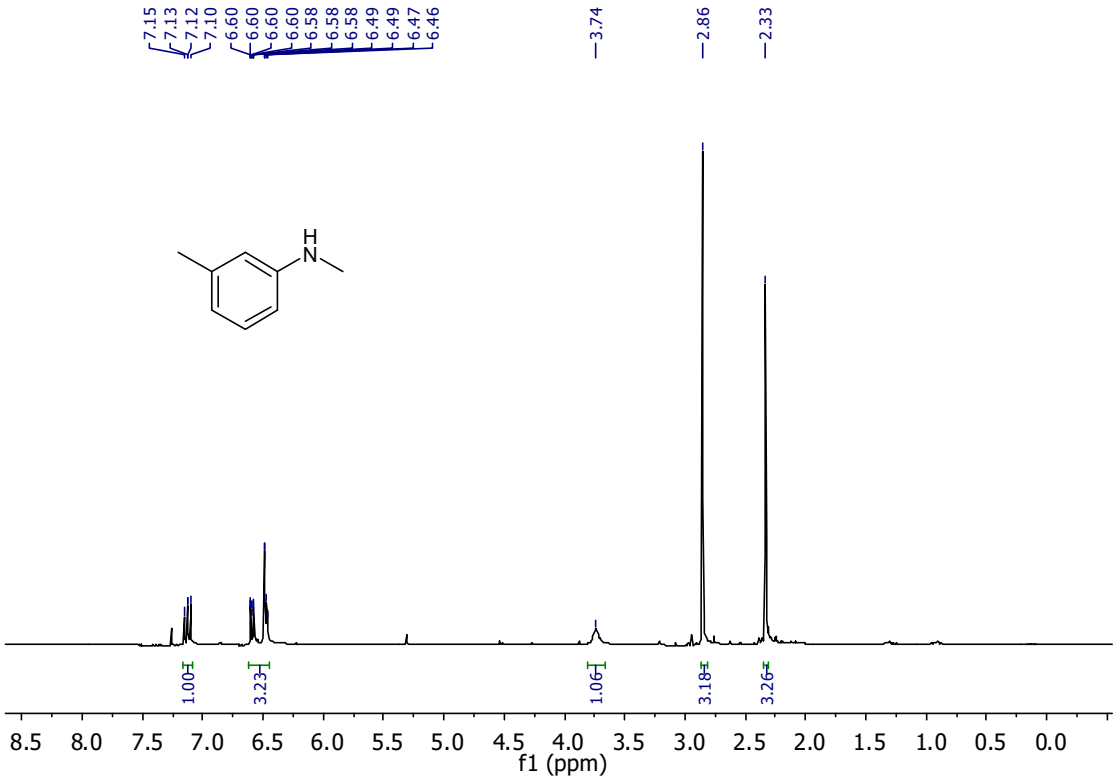

Figure S36. ^{1}H NMR of N,3-dimethylaniline.

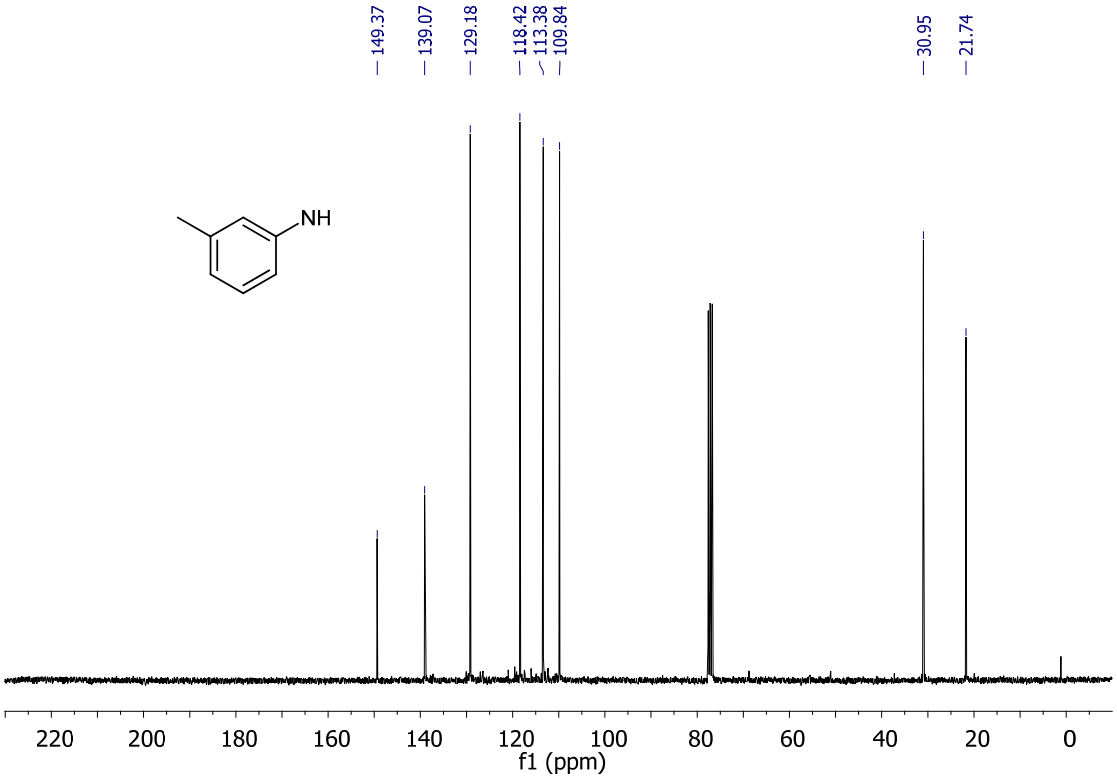

Figure S37. ^{13}C{^{1}H} NMR of N,3-dimethylaniline.

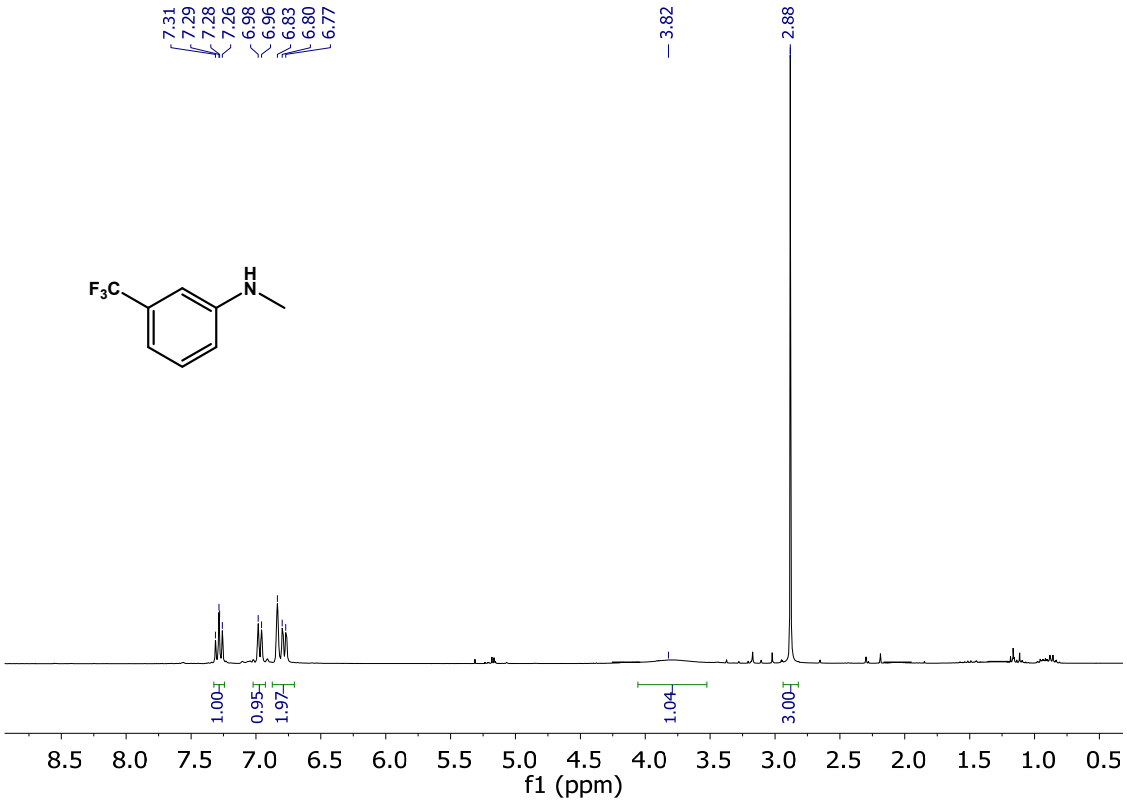

Figure S38.[1]H NMR of N-methyl-3-(trifluoromethyl)aniline.

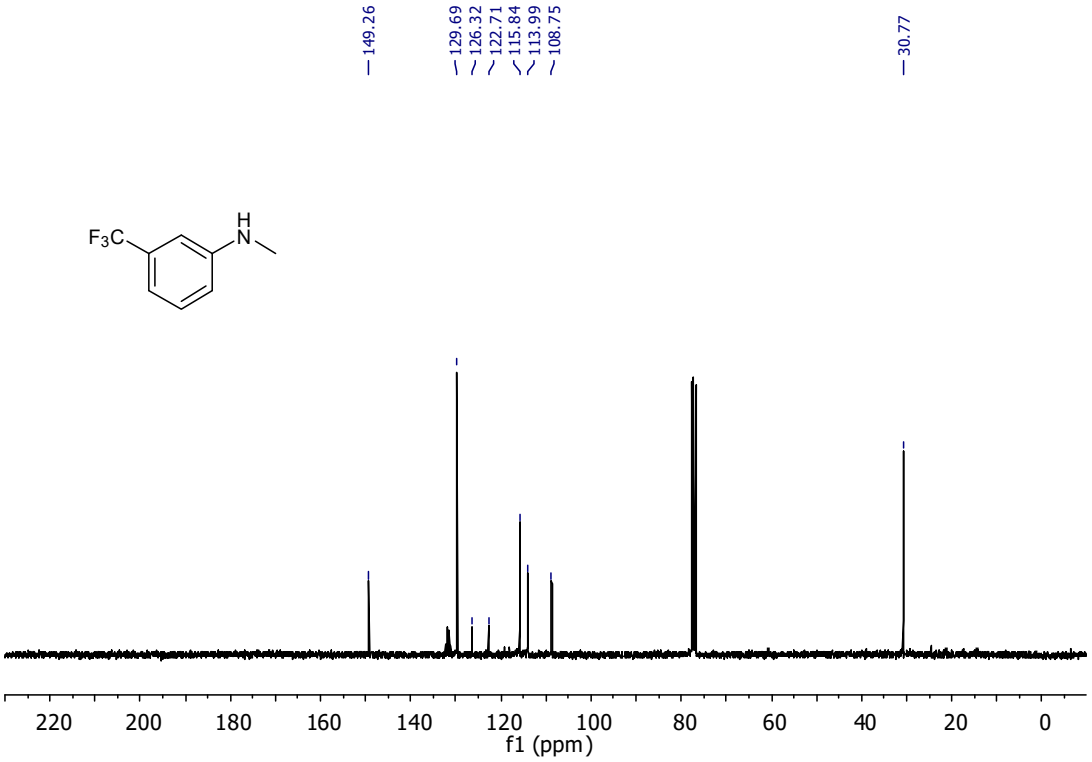

Figure S39. $^{13}C\{^{1}H\}$ NMR of N-methyl-3-(trifluoromethyl)aniline.

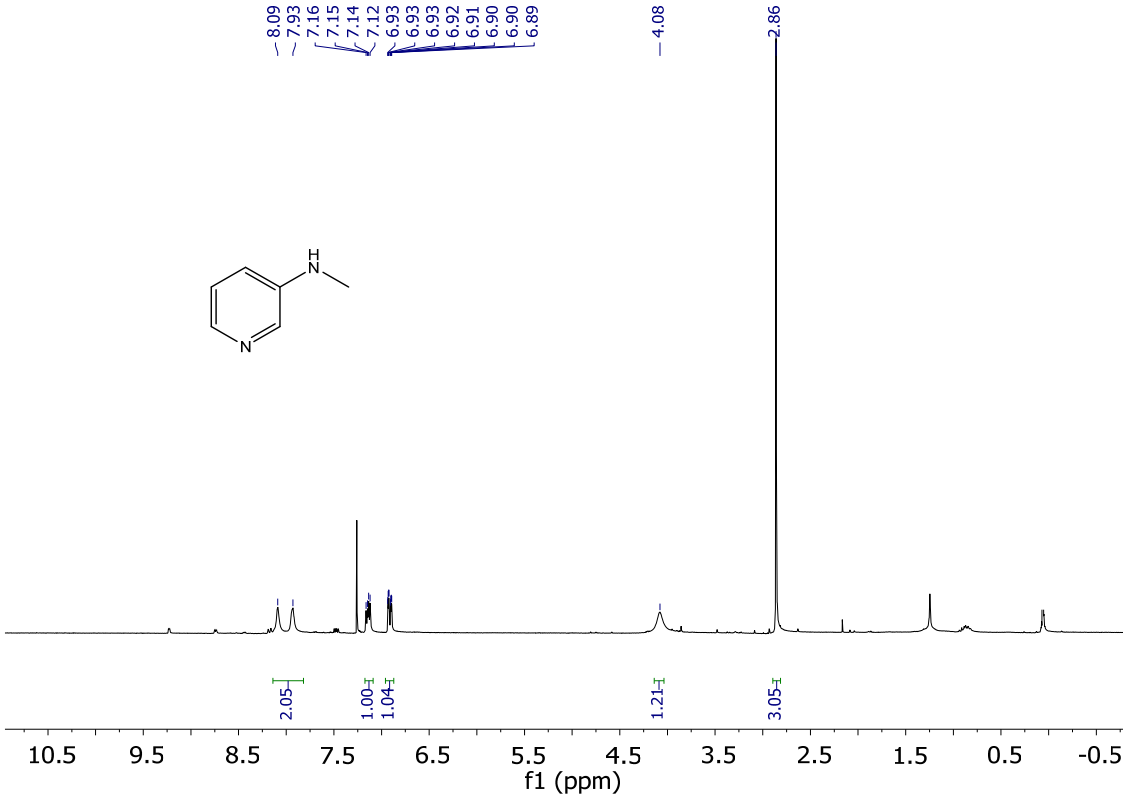

Figure S40. ^{1}H NMR of N-methylpyridin-3-amine.

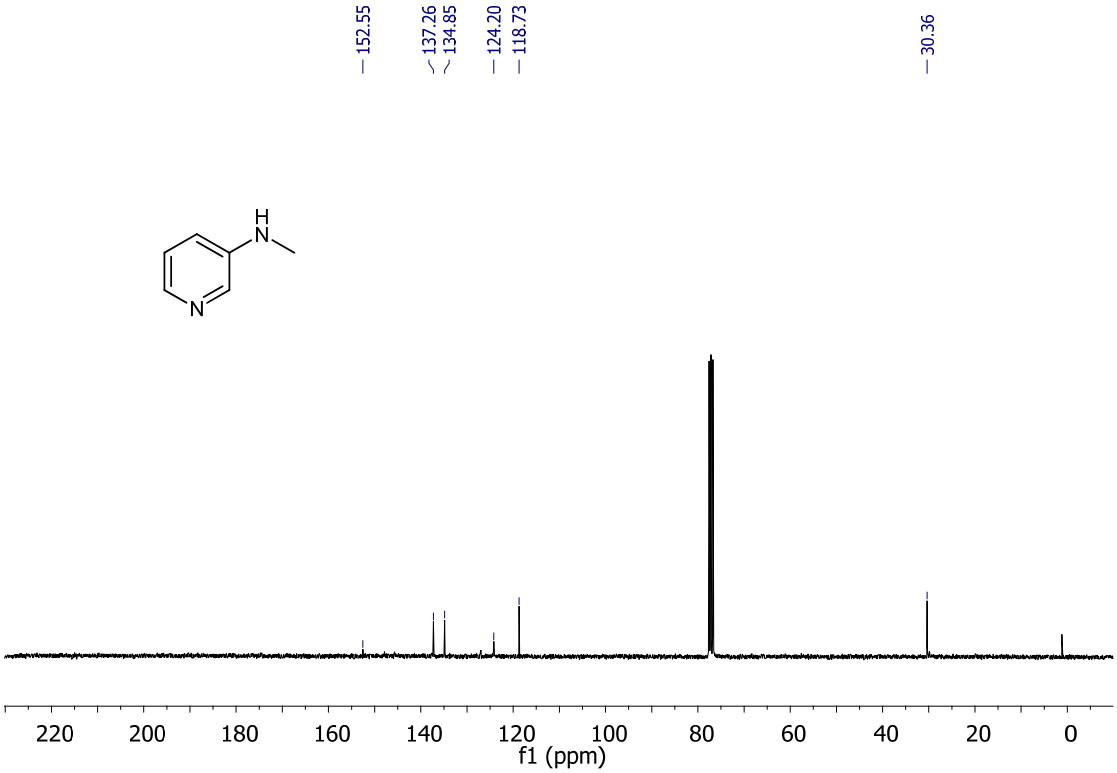

Figure S41. ^{13}C{^{1}H} NMR of N-methylpyridin-3-amine.

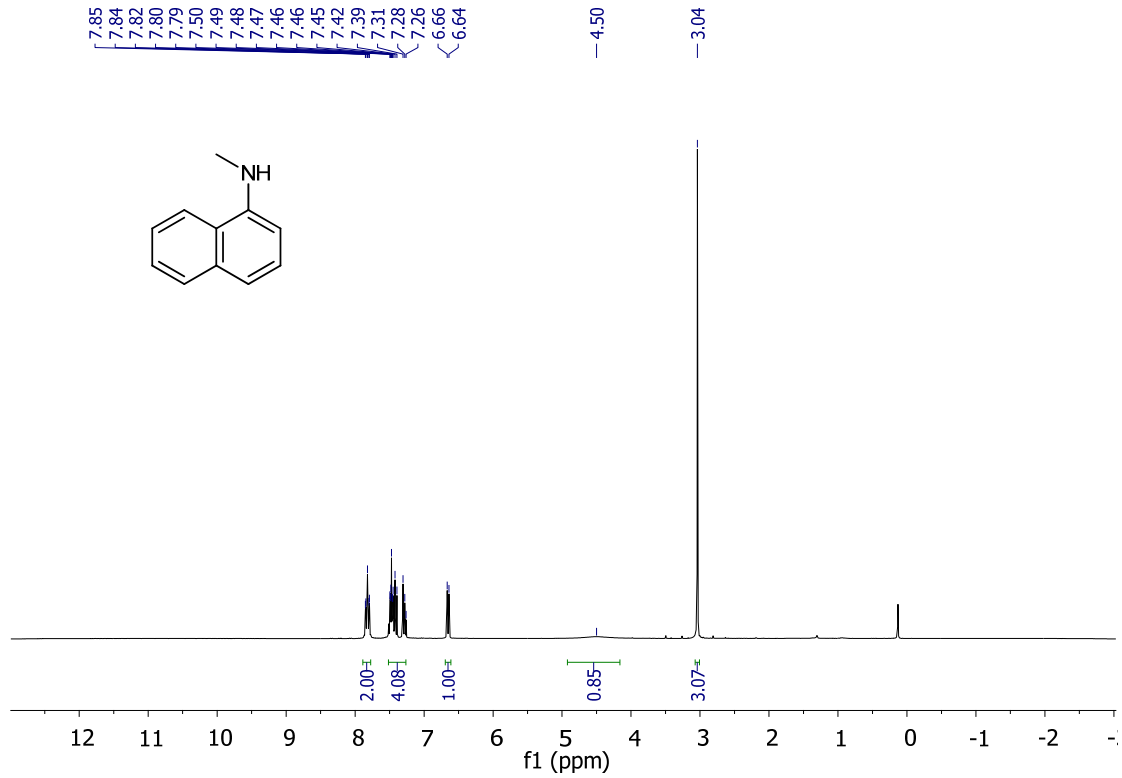

Figure S42. ^{1}H NMR of N-methylnaphthalen-1-amine.

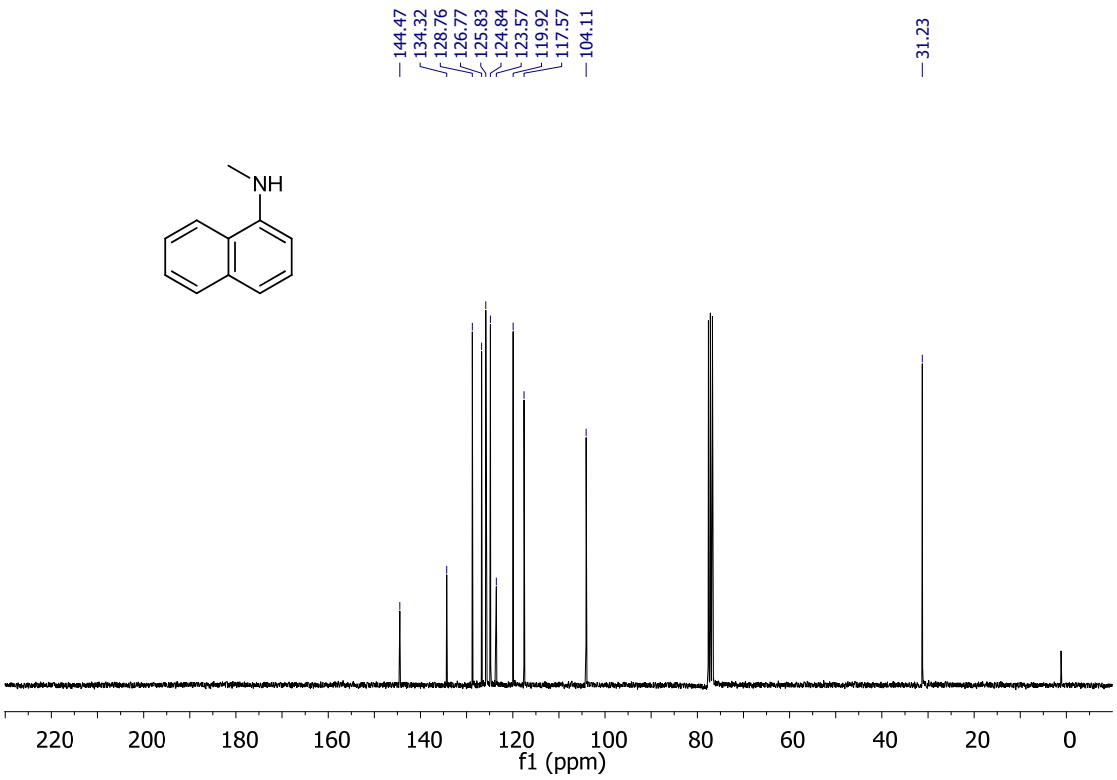

Figure S43. ^{13}C{^{1}H} NMR of N-methylnaphthalen-1-amine.

9.- References

1.- Interatomic distances have been calculated using the program PARST (Nardelli, M. *J. Appl. Crystallogr*. **1995**, *28*, 659) running under the suite WinGX (Farrugia, L. *J. Appl. Crystallogr*. **1999**, *32*, 837−838).

2.- a) Paul, B.; Shee, S.; Chakrabarti, K.; Kundu, S. *ChemSusChem* **2017**, *10*, 2370–2374. b) Wheaton, C. A.; Bow, J.-P. J.; Stradiotto, M. *Organometallics* **2013**, *32*, 6148–6161. c) Li, F.; Xie, J.; Shan, H.; Sun, C. Chen, L. *RSC Adv.* **2012**, *2*, 8645–8652.

3.- Neumann, J.; Elangovan, S.; Spannenberg, A.; Junge, K.; Beller, M. *Chem. Eur. J.* **2017**, *23*, 5410–5413.

4.- Dang, T. T.; Ramalingam, B.; Seayad, A. M. *ACS Catal.* **2015**, *5*, 4082–4088.

5.- Sun, N.; Wang, S.; Mo, W.; Hu, B.; Shen, Z.; Hu, X. *Tetrahedron* **2010**, *66*, 7142–7148.